VOLUME 35 JULY 1957 NUMBER 7

Canadian Journal of Physics

Published by THE NATIONAL RESEARCH COUNCIL
OTTAWA CANADA

CANADIAN JOURNAL OF PHYSICS

(*Formerly Section A, Canadian Journal of Research*)

Under the authority of the Chairman of the Committee of the Privy Council on Scientific and Industrial Research, the National Research Council issues THE CANADIAN JOURNAL OF PHYSICS and five other journals devoted to the publication, in English or French, of the results of original scientific research. Matters of general policy concerning these journals are the responsibility of a joint Editorial Board consisting of: members representing the National Research Council of Canada; the Editors of the Journals; and members representing the Royal Society of Canada and four other scientific societies.

Manuscripts for publication should be submitted to Dr. Léo Marion, Editor-in-Chief, Canadian Journal of Physics, National Research Council, Ottawa 2, Canada.

(For instructions on preparation of copy, see **Notes to Contributors** (inside back cover).)

Proof, correspondence concerning proof, and orders for reprints should be sent to the Manager, Editorial Office (Research Journals), Division of Administration and Awards, National Research Council, Ottawa 2, Canada.

Subscriptions, renewals, requests for single or back numbers, and all remittances should be sent to Division of Administration and Awards, National Research Council, Ottawa 2, Canada. Remittances should be made payable to the Receiver General of Canada, credit National Research Council.

The journals published, frequency of publication, and prices are:

Canadian Journal of Biochemistry and Physiology	Monthly	$3.00 a year
Canadian Journal of Botany	Bimonthly	$4.00 a year
Canadian Journal of Chemistry	Monthly	$5.00 a year
Canadian Journal of Microbiology	Bimonthly	$3.00 a year
Canadian Journal of Physics	Monthly	$4.00 a year
Canadian Journal of Zoology	Bimonthly	$3.00 a year

The price of single numbers of all journals is 75 cents.

Canadian Journal of Physics

Issued by THE NATIONAL RESEARCH COUNCIL OF CANADA

VOLUME 35 JULY 1957 NUMBER 7

THE AGING OF EVAPORATED SILVER FILMS[1]

R. A. AZIZ AND G. D. SCOTT

ABSTRACT

The spontaneous aging of thin films of silver was studied by following electrical resistance variations with time immediately after deposition *in vacuo*. In one series of experiments films, all deposited in a fixed time of 100 seconds and with initial resistances from 170,000 Ω to 20 Ω, were investigated. The resistance of some films rose rapidly with time; in others it dropped rapidly, and in still others resistance changes were less pronounced. In a second series eight films were formed, all with equal initial resistances (5000 Ω) but deposited in different times. The rate of decrease in resistance was greater as the rate of deposition increased. The limiting value of resistance depended on the time of deposition. A possible qualitative explanation of the results on the basis of distortion decay and film aggregation is proposed.

INTRODUCTION

Many workers have observed irreversible changes in the electrical resistance of evaporated metallic films. These changes can occur spontaneously at a given temperature immediately after deposition, or can be caused by temperature annealing or by chemical reactions. For those films whose resistances decrease in value, the resistance change is, at first, quite rapid and then becomes gradually slower until it is negligible. That is, the decrease in resistance with time is found to be nearly hyperbolic. The observed rapid fall can be renewed by raising the temperature to a new constant value (Vand 1936; Mitchell 1938). The phenomena are also associated with sputtered metallic films.

Mitchell (1938) observed abrupt steps in the resistance fall with time at constant temperature, each step being hyperbolic in form. This behavior has not been recorded by other workers. Reynolds and Stilwell (1952), working with copper and silver at high rates of deposition, also observed large aging effects immediately after deposition; the resistance was found to reach an approximate equilibrium in 1 to 2 hours. The films, stored in dry air, were found to remain essentially constant in resistance over a period of many months. No graphs, however, were given to illustrate the exact behavior of the films formed under definite conditions.

Mostovetch (1953) claims the existence of several variables affecting the aging of metallic films. He has found that the stability depends on the nature of the substrate and of the metal, the relative thickness of the deposit, the pressure in the evaporation chamber, the rate of deposition, and other factors. Chemical reactions are of second order provided the deposits are kept *in vacuo*.

[1]Manuscript received February 25, 1957.
Contribution from the Department of Physics, University of Toronto, Toronto, Ontario.

In view of the uncertainty of the values of resistance immediately after deposition and for some time thereafter, a systematic determination of the behavior of the films was undertaken. This study might, in addition, shed further light on the mechanism of film formation.

EXPERIMENTAL

The films were formed by thermal evaporation *in vacuo*. They were deposited on glass substrates, 8.0 mm. in length and 6.0 mm. in width, and were provided with thickly evaporated silver electrodes. Insulated leads were brought through the evaporation chamber walls. Contact to the silver electrodes was made by means of aluminum foil and copper clips. To prevent any possible effects on the resistance of the films from extraneous electrostatic fields, a grounded copper screen box was constructed about the glass support. In all runs, the substrate was subjected to a final glow discharge cleaning treatment; the evaporations were performed at a pressure of 10^{-5} mm. of Hg with a liquid air trap present in the system.

Two series of experiments were undertaken to study the problem of film aging. In the first series, films were produced at different absolute rates but with a fixed time of deposition (approximately 100 seconds). In the second series, films were formed with a given initial resistance (5000 Ω) at various rates of deposition.

In the first series, an ohmmeter (Simpson Multimeter Model 260) and a stop watch were used to measure resistance and time while the film was *in vacuo*. The effect of the applied voltage resulting from the presence of the ohmmeter in the circuit (on film aging during the deposition and afterwards) was found to be negligible. The ohmmeter, therefore, was kept in the circuit continuously from the commencement of deposition.

In the second series, automatic recording, not previously attempted by other workers, was used in order to follow rapid changes in film resistance immediately after deposition. A Brown Potentiometer Recorder with a time constant of 2.0 seconds and a full scale reading of 50 millivolts indicated the potential difference across the film as its resistance changed. The actual circuit is shown in Fig. 1A. A potential difference of 50 millivolts developed

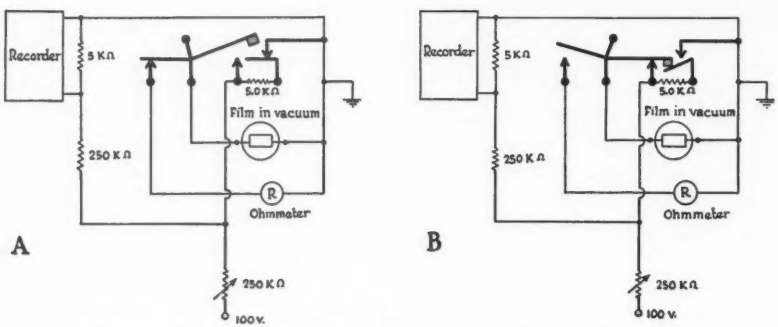

FIG. 1. Circuit used to record changes in electrical resistance of evaporated silver films.

across a fixed resistance of 5.0 kΩ maintained the recorder at full scale deflection during the evaporation. As soon as the resistance of the film reached 5.0 kΩ as indicated by the Simpson meter, the switch was thrown and simultaneously the evaporation was terminated by means of a shutter between the substrate and the atomic source. At that point, Fig. 1B was applicable. The fixed 5.0 kΩ resistor and the Simpson meter were cut out of the circuit and, at the same time, the Brown recorder was connected across the silver film of resistance of 5.0 kΩ. The recorder then followed quite linearly the change in film resistance as soon as the deposition was completed.

RESULTS

Fig. 2 indicates the resistance–time curves for several films with widely

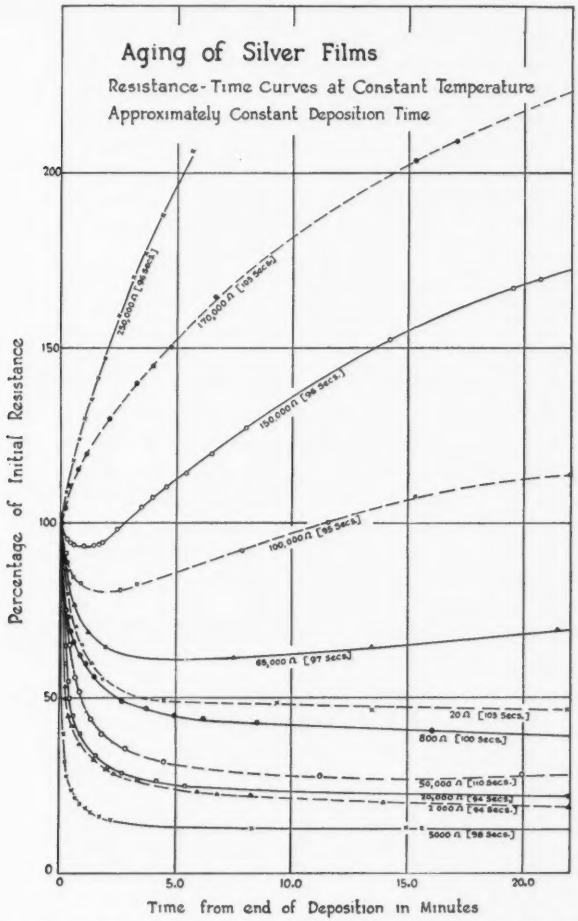

FIG. 2. Percentage change of resistance with time for films of different initial resistance.

different initial resistances, all deposited in approximately the same period of time, namely 100 seconds. The resistance is shown as a percentage of its initial resistance, R_0, at the instant deposition ceased and for a time of 22.0 minutes thereafter. The film thicknesses vary from 130 Å to 160 Å.

Films with a high resistance, R_0, e.g., 250 kΩ and 170 kΩ, increased in resistance after deposition; the greater the value of R_0, the greater was the rate of increase in resistance. The resistance of films with a lower R_0, e.g., 150 kΩ and 100 kΩ, dropped rather gradually at first, tended to become constant in value, and then rose to a point higher than R_0. As the values of R_0 became lower, the drop in resistance was more rapid and the percentage drop was larger. The trend continued until the value of R_0 was in the vicinity of 5000 Ω. At this point a crossover occurred. A film with a lower and lower R_0 decreased in resistance at a slower and slower rate, and its percentage resistance drop became less and less.

A series of eight resistance–time curves as traced out by the Brown recorder is shown in Fig. 3. Eight films with equal initial resistances of 5.0 kΩ were produced in different times of deposition. The film thicknesses range from

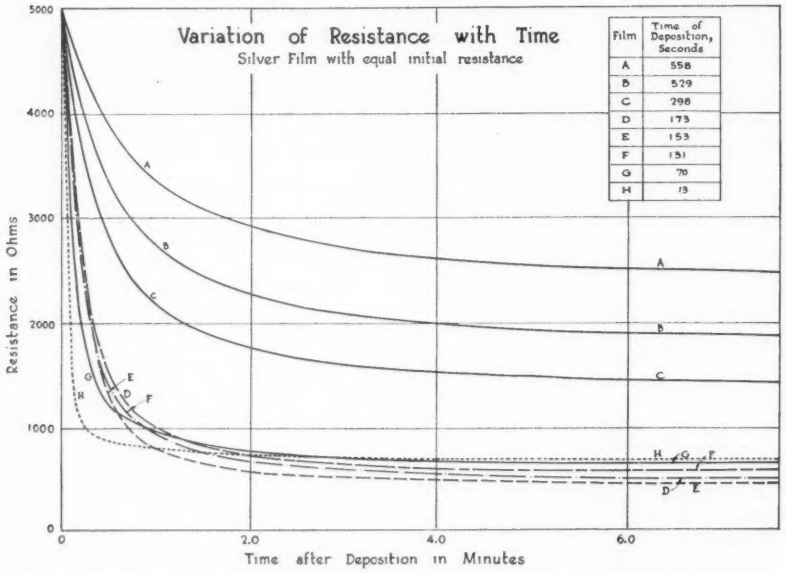

FIG. 3. The aging of silver films of the same initial resistance but deposited at different rates of evaporation.

80 Å to 180 Å. It will be noted that the faster the film was produced, the sharper was the drop in resistance. The limiting resistance decreased as the time of deposition decreased so long as the latter was above 153 seconds. At this stage a crossover took place. As the time of deposition decreased further, the limiting resistance increased.

Occasionally, some peculiar effects were observed for a rapidly produced film with an initial resistance greater than 1000 Ω. In one effect, erratic oscillations were noted in the resistance of a film even under high vacuum. The oscillations did not seem to be due to the state of purity of the silver, poor electrical contact with the film, external r-f. disturbances, or possible sensitivity to light. Another unusual effect was one similar to that observed by Mitchell (1938). The resistance dropped rapidly at first and then slowly approached a constant value. After some time the resistance fell spontaneously, tracing out a resistance–time curve as before. A series of such steps might occur until the limiting resistance neared that of an apparently identical "normal" film whose decay curve consists of the usual single step. In such films these steps could be triggered by turning on and off the variac used to control the heater current or the Philips-type ionization gauge.

DISCUSSION

Thick Films

Resistance changes can probably be explained by a gradual ordering of the crystal lattice. During condensation the atoms lose much of their kinetic energy by inelastic impact. Although the atoms are mobile on the surface, they have insufficient mobility to form a distortion-free lattice. They collide with one another, forming non-mobile Frenkel doublets, or find the nearest potential hole on the surface either of the substrate or of the metal already condensed. The positions assumed may not correspond to their place in a normal lattice. The resulting distortions in the lattice will be more prevalent when the rate of deposition is high or the velocity of the incident atoms (Aziz and Scott 1956) is low. This is due to the fact that in both cases the mobility of atoms on the surface is further lessened.

According to Matthiessen's rule, the resistance of most metals is the sum of two terms, R_T and R_D. R_T is due to the scattering of conduction electrons by thermal oscillation of the lattice. This term would be practically zero at 0° K. R_D is called the residual resistance and arises from scattering of conduction electrons on lattice distortions including impurities and boundaries of the film. This term would be zero for perfect metallic crystals infinite in size. The decrease in resistance in thick films can be explained by a decay of lattice distortions.

Vand (1943) has theorized on the mechanism of decay of distortions in metals. He has classified distortions into three groups:

(1) lattice deficiency, e.g., Schottky defects,
(2) lattice excess, e.g., interstitial atoms,
(3) combined types, e.g., imperfectly fitting surfaces of adjacent crystals embedded between bigger ones.

The first two can disappear only by means of large-scale diffusion to the surface or by meeting each other if present together. The third, however, can disappear by small-scale diffusion. Vand has theorized that small-scale diffusion is more probable as the mechanism of distortion decay and his experimental results bear this out. Aging then is due mainly to the decay of the combined type of distortion.

Each combined distortion has a higher energy content than the same number of atoms in an ordered infinite lattice. If one of its atoms, by a local random rise of temperature, reaches a certain critical value of kinetic energy, E, the decay of the distortion, i.e., an ordering process, is initiated with a liberation of energy and consequent local heating. The decay will continue until the whole distortion reaches the lowest state of energy. Each distortion has its own characteristic decay energy, E, which can vary from zero to values comparable with the height of the potential barrier for self-diffusional exchanges of atoms in the lattice.

Thinner Films

An increased rate of deposition or a decreased incident velocity (Aziz and Scott 1956) will lower the surface mobility of the silver atoms. If the surface mobility is decreased, then the probability of attachment of an atom to an abnormal surface or lattice site is increased. The density of imperfections and hence the energy content of the film (as compared to that for the same number of atoms in an ordered lattice) will then be higher. We can then expect a greater rate of decay of the imperfections or distortions. In addition, if the film is thin, the relative influence of surface forces in preventing ordering of the lattice is greater and thus contributes to high imperfection density. In very thin films, however, another phenomenon takes place, namely aggregation. Aggregation may be spontaneous in very thin films at room temperature or may be induced by temperature annealing even in thicker films. As aggregation takes place, the resistance increases. We have then two processes, spontaneous lattice ordering and spontaneous aggregation, which lead to opposing effects on the electrical resistance.

Another factor contributing to lattice distortions is the presence of occluded or trapped gas. Consider films deposited in a fixed time at a given pressure. The percentage of occluded gas will be less in thicker films where the deposition rate is higher.

On the basis of this proposed mechanism, we can explain the behavior of the curves in Fig. 2. For a given deposition time, the thickness will be somewhat proportional to the rate of deposition. In very thin films aggregation is more pronounced than lattice ordering; hence the resistance rises. The rate of rise is greater for thinner films (higher R_0). In thicker films, e.g., $R_0 = 100{,}000\ \Omega$, the relative influences of ordering and aggregation are nearly equal; the aging effects are less marked. In still thicker films ordering is of more importance and the resistance drops. The rate and extent of drop are greater as the thickness (i.e., deposition rate) increases. Then a crossover occurs. Because of the smaller influence of surface forces and the lower percentage of occluded gas, the rate and amount of the resistance decrease of thicker films lessen.

The curves of Fig. 3 can also be explained on the same basis. The films have equal initial resistances, but are formed at different absolute rates of deposition. The surface mobility of slowly produced films (thicker films) is higher; hence a more ordered film which ages more slowly and less extensively is likely to result. Besides, decay is taking place while the film is being formed.

The greater the rate of deposition (thinner films), the greater is the rate of aging, and the greater the percentage resistance drop. This state of affairs continues until the influence of aggregation reverses the trend. Therefore a crossover takes place.

Abnormal Films

The conduction electrons due to the resistance measuring device follow the chains of aggregates wherever possible. During the process of aging, chains may break while other conducting paths form. Hence we have an oscillating value of resistance.

REFERENCES

Aziz, R. A. and Scott, G. D. 1956. Can. J. Phys. **34**, 371.
Mitchell, H. R. 1938. Phys. Rev. **53**, 250.
Mostovetch, N. 1953. Ann. phys. (Paris), **8**, 61.
Reynolds, F. W. and Stilwell, G. R. 1952. Phys. Rev. **88**, 418.
Vand, V. 1936. Z. Physik, **104**, 48.
——— 1943. Proc. Phys. Soc. **55**, 222.

A CONSIDERATION OF RADIO STAR SCINTILLATIONS AS CAUSED BY INTERSTELLAR PARTICLES ENTERING THE IONOSPHERE

PART III. THE KIND, NUMBER, AND APPARENT RADIANT OF THE INCOMING PARTICLES[1]

G. A. HARROWER

ABSTRACT

In Parts I and II, as the result of an analysis of measurements of the scintillations of the radio source in Cassiopeia, it was suggested that interstellar particles, captured by the gravitational field of the Sun, contributed to the observed features. Arguments presented here lead to the conclusion that such particles must be hydrogen atoms. The number of hydrogen atoms reaching the Earth is estimated to be 6×10^{16}/m.^{2}/sec. Their energy averages 9 or 22 electron volts, depending on whether or not they are ionized. It is concluded that the effect of this infall on the Earth's ionosphere would be more than adequate to produce scintillations. The location of the radiant, subject to the possibility of some considerable error, is judged to be right ascension 17 hours, declination $-30°$. Based on this position of the radiant, the velocity of the interstellar hydrogen atoms in the vicinity of the Sun is found to have the components: tangential 28×10^4 m./sec., radial 2×10^4 m./sec., and transverse 0.2×10^4 m./sec., with respect to the plane of our galaxy.

INTRODUCTION

This is the third paper in a series concerned with the possibility of interpreting certain features of measurements of radio star scintillations in terms of the accretion of interstellar particles by the gravitational field of the Sun. The first paper (Harrower 1957*a*) presented an analysis of scintillation measurements of the radio source in Cassiopeia made at Ottawa during 1954 at a frequency of 50 megacycles per second. It was demonstrated that these measurements contained a daily variation of the maximum occurrence of scintillations which was dependent on the position of the Earth on its orbit throughout the year. This situation was accounted for in the second publication (Harrower 1957*b*) as resulting from interstellar particles, captured by the Sun's gravity and subsequently arriving at the Earth's upper ionosphere where scintillations are believed to originate. Some of these particles were thought to arrive directly from interstellar space (*F* particles), but others struck the Earth only after having entered a collision region behind the Sun (*A*, *B*, *C*, and *E* particles). It was possible to calculate from the scintillation data and the known motion of the Earth certain of these particles' velocities. It was also possible to estimate that the collision region which plays such an important part in the accretion of interstellar matter by the Sun has the shape and extent of an approximately hemispherical cap located 200 million miles from the Sun. The annual variation of the scintillation measurements was attributed to the fact that the plane of the Earth's orbit is inclined to the

[1]Manuscript received March 12, 1957.
Contribution from the Radio Observatory, Department of Physics, Queen's University, Kingston, Ontario, Canada. This work was performed in part at the Radio Physics Laboratory of the Defence Research Board under project PCC No. D48-28-01-02.

initial direction of the interstellar particles relative to the Sun in such a way that the Earth spends approximately half the year inside this hemispherical region.

In this paper it is proposed to discuss the kind of particles and their numbers arriving at the Earth, the latter with regard to the effect produced on the upper ionosphere. It will also be possible to extend the previous analysis to determine the radiant of these particles on the celestial sphere, and thereafter to describe their motion with respect to the Galaxy.

THE KIND AND NUMBER OF PARTICLES REACHING THE EARTH

1. Arguments in Favor of Hydrogen Atoms

While there is no direct experimental evidence which identifies the kind of interstellar particles believed to cause radio star scintillations, there are at least three arguments suggesting that these particles are hydrogen atoms. These arguments are based on availability, the ability to produce ionization in the upper ionosphere, and the effect of the radiation pressure of the Sun.

The availability of neutral hydrogen atoms in the interstellar space of the Galaxy is well established—both from general astronomical considerations and from recent measurements of the 21 centimeter hydrogen line. The only other matter apparently available in comparable quantity is cosmic dust. It would seem then that hydrogen atoms and cosmic dust are the only particles that should be considered from the standpoint of the amount of interstellar material being captured by the Sun's gravitational field. The case in favor of hydrogen atoms as the significant particles is strengthened by the conclusion reached by Lilley (1955), as a result of 21 centimeter measurements, that the average ratio of the spatial densities of hydrogen gas to dust in the interstellar spaces of the Galaxy is 100:1.

The height in the ionosphere at which scintillations are produced has been estimated by Hewish (1952) to be about 400 kilometers. This can provide a second argument against dust particles and in favor of hydrogen atoms. Studies of meteors have led to the conclusion that dust particles approaching the Earth do not produce appreciable ionization until they have reached their vaporization temperature; this is known to occur only at heights below 150 kilometers. Furthermore, the occurrence of scintillations of radio stars shows no maximum in the vicinity of local solar time of 0600 hours when the meteor activity is maximum. Since meteoric dust does not produce scintillations, it may be concluded that cosmic dust would be likewise ineffective. By contrast, hydrogen atoms possessing suitable energies could produce ionization in the upper ionosphere.

The third argument in favor of hydrogen atoms stems from a consideration of the effect of the radiation pressure of the Sun. Large particles possess a sufficiently large ratio of mass to surface area that radiation pressure would exert only a negligible force tending to prevent them from falling toward the Sun. However, for dust particles below a certain size (10^{-5} inch diameter, for instance) the force of radiation pressure exceeds that of gravity, and such particles could not be accreted by the Sun. Hydrogen atoms, on the other

hand, experience a force due to the Sun's radiation pressure which is only a small fraction of the Sun's gravitational force. Accordingly, the interstellar particles accreted by the Sun can safely be assumed to be hydrogen atoms.

2. The Energy of Hydrogen Atoms Arriving at the Earth

The total speed of a particle which has fallen from a very great distance to the Earth consists of three parts—the particle's initial speed v toward the Sun, and the contributions of the gravitational fields of the Earth and of the Sun. Using the value of $v = 2\times10^4$ meters per second as suggested by Hoyle and Lyttleton (1939) and calculating the other two, the resulting total speed is 4.8×10^4 meters per second. For a hydrogen atom this amounts to an energy of 12 electron volts.

If it is assumed that particles start to fall toward the Sun from the collision region with zero initial speed, the speed of those reaching the Earth is the result of the combined effects of the gravitational fields of Earth and Sun. The speed of an A particle, calculated in this way, is 3.3×10^4 m./sec., which is equivalent to an energy of 5.7 ev.

An F or A particle reaching the Earth may have, in addition to the energies calculated above, an energy of ionization. The Sun's ultraviolet radiation could ionize incoming hydrogen atoms, thereby giving them an additional energy of 13.5 ev. This would bring the total energies of F and A particles to 25.5 ev. and 19.2 ev. respectively.

3. The Effects of Incoming Particles on the Earth's Ionosphere

The possibility of these incoming particles producing an observable effect on the Earth's upper ionosphere obviously depends on the number of particles arriving. An estimate of this number can be obtained by using Hoyle and Lyttleton's expression (1939) for the mass accreted by the Sun per second, which is $4\pi G^2 p M^2/v^3$, in which G = gravitational constant = 6.7×10^{-11} nt.m.^{2}/kg.^{2}, p = density of interstellar matter = 10^{-15} kg./m.^{3}, M = mass of Sun = 2×10^{30} kg., v = velocity of Sun relative to interstellar matter = 2×10^4 m./sec., where the p and v values are those suggested by Hoyle and Lyttleton. The result is a rate of accretion of interstellar matter by the Sun of 2.8×10^{13} kg./sec., which represents 1.7×10^{40} hydrogen atoms/sec. Now, if it is assumed that this infall of particles is uniformly distributed over a sphere of radius 93 million miles, the Earth would receive interstellar particles on its outward surface at the rate of 6.0×10^{16} particles/m.^{2}/sec. Taking the speed of these particles arriving at the Earth to be 4×10^4 m./sec. (the average of the A and F particle speeds from Part II), this infall consists of 1.5×10^{12} hydrogen atoms/m.^{3}

The significance of this result can be judged by comparing it with the 10^{12} ions/m.^{3} estimated to exist normally at an altitude of 400 km. (Mitra 1952, p. 288). Thus, if all the incoming hydrogen atoms are ionized, they would increase the normal density of ionization by 150%. On the other hand, even if all the particles arriving are neutral hydrogen atoms, they would produce a not insignificant change in the ionization density. For an estimated density

of gas at the 400 km. altitude of 1.1×10^{14} atoms/m.^{3} (Mitra 1952, p. 3), this infall of neutral hydrogen atoms would change the density of ionization by about 1.5%. Ryle and Hewish (1950) estimate that 0.1% changes in ionization density would suffice to cause the scintillation of radio stars. The simple calculations just performed, then, show that the supply of particles resulting from the accretion of interstellar hydrogen atoms by the Sun is adequate to support the explanation, here being put forth, for certain features of the scintillation measurements.*

LOCATION OF THE RADIANT OF PARTICLES AND THEIR MOTION IN OUR GALAXY

1. Procedure for Finding the Radiant

The motion of the interstellar particles relative to the Sun determines the point on the celestial sphere from which they appear to originate as would be seen from the Sun, or from the Earth after correction for the Earth's orbital motion. Fig. 1(*a*) shows the celestial sphere with the Sun at its center

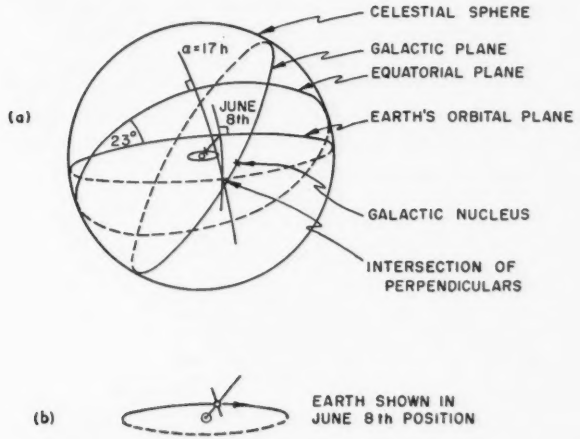

FIG. 1. The celestial sphere is shown with the Sun at the center and the Earth on its orbit around the Sun. Part (*b*) shows the Earth in the same position on its orbit as does (*a*), but to a larger scale. The seasonal and daily variations revealed in the scintillation measurements allow the position of the radiant of incoming particles to be determined. Perpendiculars erected on the surface of the celestial sphere at the June 8 position on the Earth's orbital plane and at right ascension 17 hours on the Earth's equatorial plane intersect at the radiant. Thus, the radiant is slightly above the galactic plane and near the galactic nucleus.

and the Earth on its orbit around the Sun. Three planes are shown in the figure, which are the orbital and equatorial planes of the Earth (meeting at an angle of 23°) and the plane of the Galaxy. Scintillation data can be related to the orbital and equatorial planes as follows. Concerning the orbital plane,

*There remains the question, not answerable from these measurements or this analysis, of whether the ionization is produced in an irregular pattern (irregular, at least, to the extent of 0.1%) or whether it becomes irregular after production, possibly by the action of turbulence.

the Earth has been found to be on the forward side of the Sun (the side on which interstellar particles arrive) on June 8. This means that the radiant of particles must lie on a perpendicular on the surface of the celestial sphere erected at the June 8 position of the Earth on its orbit. This particular position of the Earth is shown in enlarged scale in Fig. 1(*b*). The location of the radiant with respect to the equatorial plane can be determined from the local solar time of maximum scintillation on June 8. The scintillation referred to here is, of course, that attributed to the direct infall of interstellar particles (the *F* particles of Part II), rather than that due to particles from the collision region behind the Sun. The measurements showed a maximum in this scintillation activity at approximately 21.30 hours for dates of the year near June 8 (Part II, Fig. 9). This was based on the assumption of an initial velocity of interstellar particles relative to the Sun of 2×10^4 m./sec. This assumption and the necessity of applying some correction for the effect of the Earth's magnetic field introduce the possibility of a rather large error in the subsequent calculations. A simple correction for the Earth's magnetic field can be based on the fact that the time 21.30 hours and date June 8 locate the radiant, as seen from Ottawa, near the southern horizon. Under such conditions, the incoming particles move northward at a small angle to the Earth's surface and will be deflected by the Earth's magnetic field. A comparison of the lines of magnetic longitude with lines of geographic longitude shows that incoming charged particles would veer westward. The result of this is that such particles would have maximum effect on the ionosphere near Ottawa approximately 2 or $2\frac{1}{2}$ hours earlier than would be the case if the Earth's magnetic field were absent. If the time 21.30 hours is corrected to approximately 23.45 hours, this may be used in determining the direction of arrival of the interstellar particles. The corresponding value for the right ascension is 17 hours and at this point on the equatorial plane in Fig. 1(*a*), a perpendicular is shown on the surface of the celestial sphere. The intersection of this perpendicular with the one previously erected locates the radiant of the incoming particles. The coordinates of the radiant are judged to lie within right ascension 16 hours 40 minutes to 17 hours, and within declination $-20°$ to $-40°$.

2. Particles' Motion with Reference to the Plane of the Galaxy

The radiant just found is close to the center of the Galaxy. This was shown in Fig. 1(*a*) and is depicted from a different viewpoint in Fig. 2. In the latter figure, a section of the galactic plane is shown, including the galactic center and the Sun in motion around the center. The radiant is separated by about 7° from the center and is about 5° above the galactic plane as seen from the Sun. Knowledge of these angles allows the relative sizes of the components of the particles' velocity—radial, transverse, and tangential to the galactic plane—to be derived. As before, the particles' velocity from their radiant toward, and relative to, the Sun will be assumed to be $V_A = 2\times10^4$ m./sec. Furthermore, the tangential component will be affected by the Sun's speed in its galactic orbit which is $V_s = 28\times10^4$ m./sec. The resulting components of velocity with reference to the galactic plane are as follows:

radial component $= V_A \cos 7° = 2\times10^4$ m./sec.,

transverse component $= V_A \sin 5° = 0.2\times10^4$ m./sec.,

tangential component $= V_s + V_A \sin 5°$

$=$ slightly more than 28×10^4 m./sec.

The ratio of these quantities is seen to be 10:1:140.

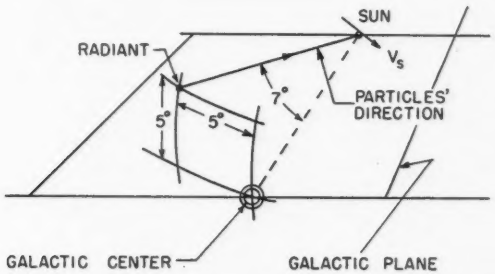

FIG. 2. The motion of the interstellar particles believed to contribute to scintillations is more easily visualized, with reference to our galaxy, from this viewpoint. A section of the galactic plane is shown with the Sun moving with speed V_s in its orbit around the galactic center. The position of the radiant is indicated approximately.

CONCLUSION

Beginning herein with the idea, previously presented, that some features of the measurements of the occurrence of scintillations of radio stars can be accounted for as resulting from the capture of interstellar particles by the gravitational field of the Sun, the questions of the nature of the particles involved, their effect on the Earth's ionosphere, and their direction of arrival have been examined. The conclusions are that such particles must be hydrogen atoms and that they arrive at the Earth in sufficient number and with adequate energies to produce the ionospheric conditions believed necessary for the occurrence of scintillations. Their radiant has been found (subject to the possibility of some sizable errors) and this has allowed the particles' motion relative to our galaxy to be calculated. This motion consists principally of a tangential component only slightly greater than the Sun's orbital speed, so that the hydrogen atoms overtake the Sun in their orbital motion around the galactic center. In addition, they move radially outward from the galactic center and possess a very small component of velocity transverse to the galactic plane. Within the limitations imposed by possible errors in the location of the radiant, then, this description applies to the motion of interstellar hydrogen atoms in the vicinity of our Sun.

The analysis of daily and seasonal variations in the scintillation data which led to the presentations made in Parts I, II, and III of this series also revealed effects attributable directly to the Sun. These will be discussed, at a later date, in the final Part IV.

REFERENCES

HARROWER, G. A. 1957*a*. Can. J. Phys. **35**, 512.
——— 1957*b*. Can. J. Phys. **35**, 522.
HEWISH, A. 1952. Proc. Roy. Soc. A, **214**, 494.
HOYLE, F. and LYTTLETON, R. A. 1939. Proc. Cambridge Phil. Soc. **35**, 405, 592.
LILLEY, A. E. 1955. Astrophys. J. **121**, 559.
MITRA, S. K. 1952. The upper atmosphere (Asiatic Society, Calcutta).
RYLE, M. and HEWISH, A. 1950. Monthly Notices Roy. Astron. Soc. **110**, 381.

ON THE SPECIFIC HEAT OF SOLIDS AT LOW TEMPERATURES[1]

T. H. K. Barron[2] and J. A. Morrison

ABSTRACT

The temperature dependence of the specific heat of solids at very low temperatures is examined, using theoretical models and certain recent experimental results. The temperature region over which the continuum approximation ($C_v = aT^3$) is strictly reliable is shorter than has often been supposed, and the series expansion $C_v = aT^3+bT^5+cT^7+\ldots$ is needed for the analysis of accurate experimental results. For insulators Θ_0 can best be estimated from measured specific heats by plotting C_v/T^3 versus T^2; the result is a curve whose intercept at $T^2 = 0$ gives the coefficient of T^3 (and hence Θ_0), and whose slope and curvature give additional information about the vibrational spectrum at low frequencies. For metals the usual plot of C_v/T versus T^2 can be used, but here again neglect of curvature may lead to errors in the estimates of γ and Θ_0. A brief discussion is given of the low temperature specific heats of a number of solids for which suitable data are available: potassium chloride, lithium fluoride, white tin, tungsten, the noble metals, and elements of diamond structure.

1. INTRODUCTION

It is well known that as the absolute zero of temperature is approached the lattice specific heat of crystals should become equal to that of an elastic continuum, and should then be given by

$$C_v = aT^3. \tag{1}$$

The T^3 dependence of the specific heat depends upon the frequency spectrum's taking the form at very low frequencies

$$g(\nu) = \alpha\nu^2, \tag{2}$$

where $g(\nu)$ is the number of frequencies between ν and $\nu+d\nu$. At higher frequencies the spectrum departs from (2) and it is necessary to use the complete low frequency expansion

$$g(\nu) = \alpha\nu^2+\beta\nu^4+\gamma\nu^6+\ldots; \tag{3}$$

this leads to a corresponding series for the specific heat

$$C_v = aT^3+bT^5+cT^7+\ldots. \tag{4}$$

When the contributions of the terms in T^5, T^7, etc., are negligible, the equivalent Debye characteristic temperature, Θ_D, flattens off to a constant value, Θ_0, proportional to $a^{-1/3}$. The significance of Θ_0 is that it can also be derived from the elastic constants of the crystal; its determination, therefore, allows us to correlate thermal and mechanical properties.

In order to estimate Θ_0 from measured specific heats it is important to establish the magnitude of the coefficients b and c. Since no general prediction can be made from theory (Blackman 1937), recourse must be had to experiment. Coefficients can, of course, be worked out for specific models. From

[1]Manuscript received March 4, 1957.
Contribution from the Divisions of Pure Physics and Pure Chemistry, National Research Laboratories, Ottawa.
Issued as N.R.C. No. 4384.
[2]National Research Laboratories Postdoctorate Research Fellow.

consideration of both theory and experiment Blackman (1941) has suggested that temperatures less than $\Theta_D/50$ to $\Theta_D/100$ would have to be reached if Θ_D is to become constant within about 1%.* This has often been loosely interpreted as meaning that a perfectly constant value of Θ_D should be observed below $\Theta_D/50$; such an interpretation implies complete neglect of the terms in T^5 and T^7 in this region of temperature. But the form of equation (4) suggests that the most straightforward way of deducing a (and hence Θ_0) from experimental results is to plot C_v/T^3 versus T^2. This should yield a *curve* whose intercept with the axis at $T^2 = 0$ will be a; moreover, the slope will give b and the second derivative will give $2c$. In this way we avoid the naïve assumption of a perfectly constant Θ_D at very low temperatures.

In this paper we are chiefly concerned to see how far such an analysis can be carried out for a number of crystals for which suitable specific heat data are available. The results for two theoretical models are used to guide the analysis; in particular, they indicate the temperature region where the terms in T^5 and T^7 are likely to become significant. Since the models do not represent closely any of the experimental crystals later considered, quantitative agreement should not be expected; in fact, both theory and experiment indicate that the extent of the T^3 region depends upon the substance concerned. The analysis of experimental results shows that detectable changes in Θ_D can occur at temperatures well below $\Theta_D/50$, and that neglect of this variation can lead to appreciable errors in the estimation of Θ_0. It also becomes clear that great care must be taken in applying equation (4) since inaccuracies in measurements can easily suggest incorrect estimates of a and b; this danger is greatly enhanced when there is also an electronic contribution to the specific heat.

2. DEDUCTIONS FROM MODELS

(*a*) *General*

Before analyzing experimental results it is useful to discuss the behavior to be expected according to various theoretical models. For our purpose it is important to discuss models sufficiently simple for the low temperature behavior to be determined exactly. For this reason models representing specific substances (Bhatia and Horton 1955; Horton and Schiff 1956) are not within the scope of the present paper.

A thorough investigation has been made by Blackman (see Blackman (1956) for detailed references) of the variation of Θ_D with temperature for a number of diatomic lattices (linear, square, and cubic), with Hooke's law forces between first and second neighbors. These models all showed a common general behavior:

(i) At low and at high temperatures Θ_D flattened off to roughly constant values; these values have later been called Θ_0 and Θ_∞ respectively.

(ii) Below a temperature of $\Theta_D/100$ to $\Theta_D/50$ the total variation of Θ_D was less than 1%; Θ_D always decreased with increasing temperature in this range.

*Θ_D is not precisely defined unless the temperature is specified, but usually this does not matter when giving these rough limits. If there is a large variation in Θ_D the limits can be taken as $\Theta_0/100$ to $\Theta_0/50$.

(iii) An increase of the mass ratio (M/m) of the atoms increased Θ_∞/Θ_0 and thus tended to produce an over-all increase of Θ_D with temperature; on the other hand its effect at the lowest temperatures was to augment the rate of *decrease* of Θ_D. In most of the models these effects combined to produce a minimum in Θ_D at temperatures of the order of $\Theta_D/12$.

The possibility that the coefficient b need not always be positive was also examined (Blackman 1937), and it was found that b could indeed be negative for some values of the force constants. However, under these conditions the lattice was unstable since the force constant between second neighbors was then always negative. Since negative force constants are permissible in other lattices (e.g., between second neighbors of a face-centered cubic lattice) Blackman concluded that it was probable that no general rule could be made for the sign of b. We may conclude further that there will only be a long T^3 region in the special case where b is very small. For all of the models studied in detail b was positive and a strict T^3 region did not occur, with one apparent exception which we shall now discuss.

(*b*) *The Diatomic Linear Chain*

Blackman (1935*b*) calculated the points shown in Fig. 1(*a*) for the diatomic linear chain at low temperatures with $M/m = 8$ and $\Theta_0 = 195°$ K.; the dashed

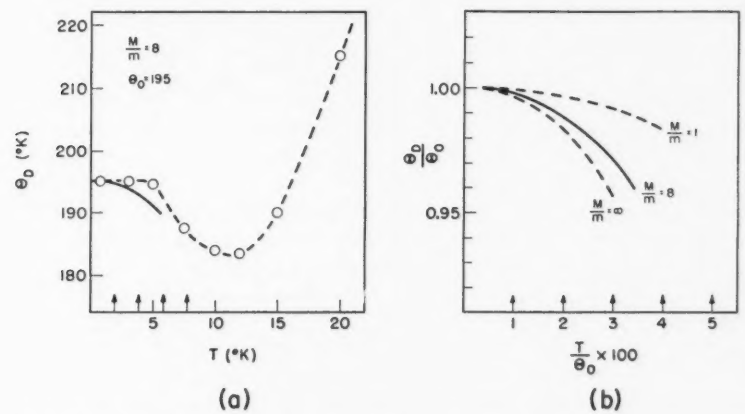

FIG. 1. Variation of Θ_D with T for a model diatomic chain. From the left the arrows on the abscissa indicate the temperatures $\Theta_0/100$, $2\Theta_0/100$, etc. (*a*) - - - O - - -, Blackman (1935*b*); ———, equation (5). (*b*) The influence of the mass ratio (equation (11)).

curve through these points gives a negligible variation of Θ_D for temperatures less then $\Theta_0/50$, followed by a sudden drop at about 5° K. This picture at first seems to confirm the impression that a strict T^3 region is to be expected from theory, contrary to the general conclusions we have just drawn. However, Blackman was concerned only to demonstrate the existence of the dip in the value of Θ_D, and not at that time to study its precise form; in his numerical

integrations he therefore aimed at an accuracy of 1%, sufficient to show the size of the dip but quite insufficient to show details of its shape below 6° K. For this we need to expand C_v (or Θ_D) in a series of powers of T; for $M/m = 8$ we find (cf. the appendix)

$$\Theta_D = \Theta_0\{1-2.78(T/\Theta_0)^2-46.9(T/\Theta_0)^4-2016(T/\Theta_0)^6-\ldots\}. \tag{5}$$

The actual behavior of Θ_D at low temperatures is then that given by the solid curve in Fig. 1(*a*). The strict T^3 region and the sudden dip in Θ_D have now disappeared, but the two curves are compatible to within about 1%. In Fig. 1(*b*) we show the variation of Θ_D/Θ_0 for $M/m = 8$, and also for the two limiting cases of equal and very unequal masses. A longer T^3 region is obtained for $M = m$ than for $M = 8m$, but there is still no sharp drop in Θ_D. The results agree with Blackman's findings that an increase of mass ratio should increase b; in particular the curve for $M/m = \infty$ is obtained by halving the abscissae corresponding to $M/m = 1$.

(*c*) *The Close-packed Cubic Lattice*

Another model suitable for discussion is provided by some recent theoretical work on the close-packed cubic lattice with central forces between nearest neighbors (Salter 1956). For this lattice we have

$$C_v = aT^3\{1+55.2(T/\Theta_0)^2+10^4(T/\Theta_0)^4+\ldots\}. \tag{6}$$

Here, the coefficient of $(T/\Theta_0)^2$ has been derived from the results of detailed calculations of a (Barron and Domb 1955) and of b (Barron 1955) and should be accurate. The coefficient of $(T/\Theta_0)^4$ is of the order of magnitude predicted by two independent approximations due to Salter (1956) and Leighton (1948); in particular, Salter's approximation agrees remarkably closely with the exact calculations for a and b.

Figure 2 is a plot of C_v/aT^3 versus $(T/\Theta_0)^2$ as given by equation (6). The solid line represents the asymptotic form aT^3+bT^5 and the arrows on the temperature axis show successive temperatures $\Theta_0/100$, $2\Theta_0/100$, etc. One sees that, as in Blackman's models, Θ_D is constant to within 1% for $T < \Theta_D/50$, and that the variation of Θ_D within this range is given very accurately by the two terms aT^3+bT^5. This suggests that for a close experimental determination of Θ_0 we need accurate measurements within this range.

A further point which must be noted is that in the range immediately above $\Theta_D/50$ experimental scatter could easily give rise to a "pseudo" aT^3+bT^5 region as shown by the dashed line in Fig. 2. This would give too low a value af a and much too high a value of b. In plotting the points of Fig. 2 we have, of course, neglected additional terms in the expansion (6), and also the effect of the subsequent fall-off in C_v/T^3 due to the cutoff of one or more branches of the frequency spectrum; the increasing influence of the cutoff might well lead to even further extension of the quasi-linear region. Experimental results discussed below reveal that such "pseudo" asymptotic regions do indeed occur, but there need usually be no confusion if it is remembered that the true asymptotic region is unlikely to extend beyond $\Theta_D/50$.

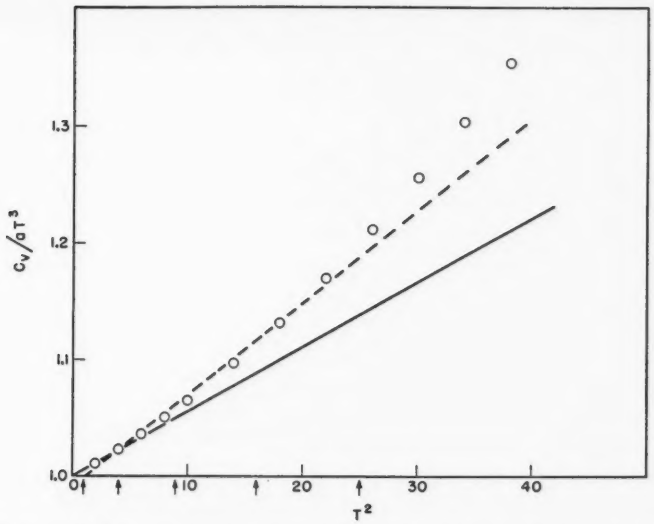

FIG. 2. A graph of C_v/aT^3 versus T^2 for a model close-packed cubic lattice (equation (6)). From the left the arrows on the abscissa indicate the temperatures $\Theta_0/100$, $2\Theta_0/100$, etc. O, calculated (equation (6)); ———, asymptote $C_v = aT^3+bT^5$; - - - - -, "pseudo" asymptote.

3. ANALYSIS OF EXPERIMENTAL RESULTS

Although there are many substances for which the specific heat has been measured at very low temperatures, the data have usually been given only in the form of graphs or of tables of smoothed values. Neither form is suitable material for detailed analysis. The discussion will therefore be restricted mainly to crystals for which the original experimental results are available.

(*a*) *Alkali Halide Crystals*

We have recently had occasion to fit equation (4) to specific heat data for five alkali halide crystals (potassium chloride, bromide, and iodide, and sodium chloride and iodide) in the temperature region $2.8° < T < 20°$ K., and have derived values of Θ_0 and rough estimates of b for each salt (Barron, Berg, and Morrison 1957). As an example we shall discuss potassium chloride, which was one of the two salts (sodium iodide was the other) for which the effect attributable to the T^7 term was most clearly observed. A second, independent example is provided by lithium fluoride. For this salt Martin (1955) and Clusius and Eichenauer (1956) have each claimed to have found a T^3 dependence of the specific heat for $T < \Theta_D/40$, although their two estimates of Θ_0 differ by 2% (or 14°).

(*i*) *Potassium Chloride*

The results are plotted in the form of C_v/T^3 versus T^2 in Fig. 3. The estimated probable error of the measurements of C_v varies from 3% at 2.8° to 1% at 4°, and then onwards decreases rapidly to 0.2% for $T \geqslant 10°$ K. (Berg and

Morrison 1957). The solid curve in Fig. 3 has been drawn with regard for these accuracies; from it we deduce $a = 7.15(\pm 0.05)\times 10^{-5}$ cal./mole deg.[4]

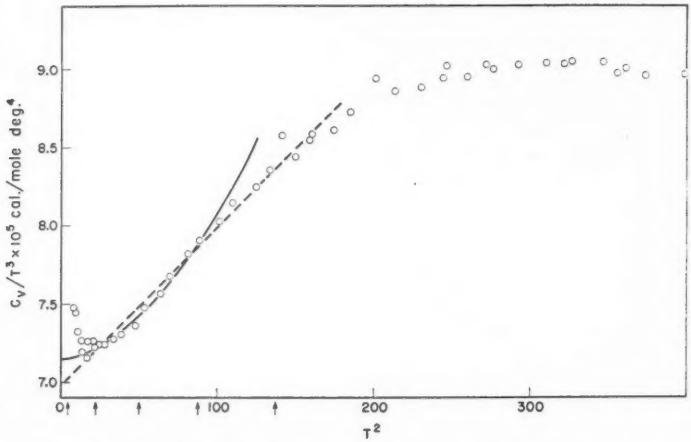

FIG. 3. A graph of C_v/T^3 versus T^2 for potassium chloride. From the left, the arrows on the abscissa indicate the temperatures $\Theta_0/100$, $2\Theta_0/100$, etc.

($\Theta_0 = 235.1(\pm 0.5)°$ K.) and $b = 3(\pm 1)\times 10^{-8}$ cal./mole deg.[6] It should be noticed that the accuracy of Θ_0 is appreciably higher than that of the experiments at 2.8° K.: knowledge of the form of the specific heat (equation (4)) enables us to deduce that the specific heats measured at the lowest temperatures are too high. The departure of the specific heat from the asymptotic form aT^3+bT^5 becomes marked for $T > \Theta_D/50$. The specific heat of potassium chloride has also been measured in the region $T < 4°$ K. by Keesom and Pearlman (1953*b*) and by Webb and Wilks (1955). Keesom and Pearlman assumed the T^3 law and give $\Theta_0 = 233(\pm 3)°$ K.; the smoothed results tabulated by Webb and Wilks lead to $\Theta_0 = 237°$ K., but also to a value of b (2×10^{-7} cal./mole deg.[6]) which is an order of magnitude larger than that given by Fig. 3.

The decreasing slope of the graph of C_v/T^3 versus T^2 for $T^2 > 100$ presumably reflects the influence of the cutoff of the frequency spectrum; this offsets the contribution of the higher terms in the low temperature expansion (equation (4)) and leads to a "pseudo" aT^3+bT^5 region (dashed line in Fig. 3) extending up to $T = \Theta_D/20$.

(ii) Lithium Fluoride

A similar graph of the results of Clusius and Eichenauer (1956) is shown in Fig. 4. As they stand, the results suggest that the coefficient b is zero, in marked contrast with the results for the other alkali halides. Although such a contrast cannot be definitely ruled out, there are reasons for believing that the results do not give a wholly correct picture. In the first place the mass ratio is appreci-

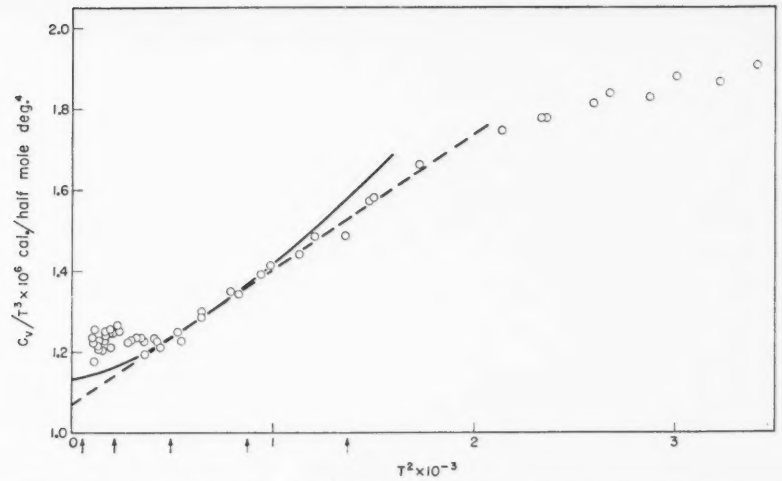

FIG. 4. A graph of C_v/T^3 versus T^2 for lithium fluoride—data of Clusius and Eichenauer (1956). From the left, the arrows on the abscissa indicate the temperatures $\Theta_0/100$, $2\Theta_0/100$, etc.

ably different from unity; this would be expected to increase b, not to decrease it. Still more important, the C_v/T^3 versus T^2 plot shows a very sharp curvature in the neighborhood of $T = 3\Theta_0/100$, which is hard to accept since it is not observed in any of the other alkali halides. We would suggest, therefore, that the behavior of the specific heat below 20° K. is probably more like that shown by the solid curve in Fig. 4, which has been obtained by extrapolating the results for $T > 20°$ K. in accordance with the general trend observed in the other alkali halides. This agrees reasonably with Martin's results (Fig. 5) and leads to $\Theta_0 = 743°$ K., rather than to 723° K. as suggested by Clusius and Eichenauer. As with potassium chloride a "pseudo" aT^3+bT^5 line can be drawn (dashed line in Fig. 4) which would indicate too high a value of Θ_0 (757° K.).

The elastic constants of lithium fluoride have recently been measured down to 4° K. by Briscoe and Squire (1957), and give $\Theta_0 = 743°$ when de Launay's tabulated functions (de Launay 1956) are used for the calculation of Θ_0; such good agreement with the value deduced from the specific heats must be in part fortuitous. Briscoe and Squire derived a value of 775° K. for Θ_0 from their results, but this estimate was obtained by an approximate method much less accurate than de Launay's tables.

(b) Metals and Semiconductors

For insulators at low temperatures we have only to consider the contribution of the lattice vibrations to the specific heat, which is known to take the form of equation (4). For metals and semiconductors we have also to consider the contribution of the "free" electrons, and strictly speaking this is not

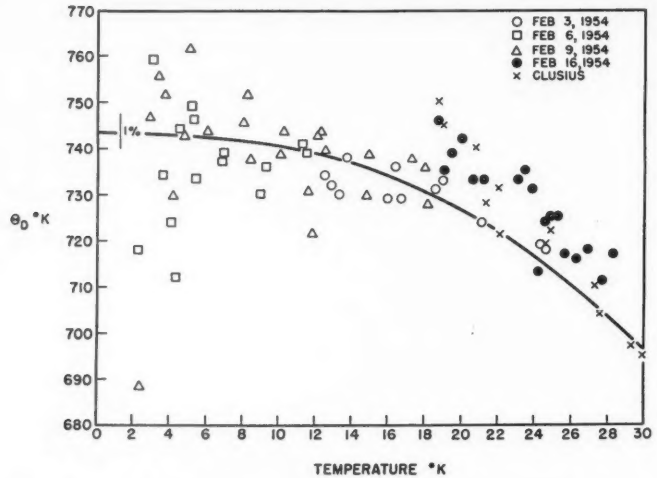

FIG. 5. A comparison of Martin's experimental results (Martin 1955, Fig. 1; reproduced by courtesy of *The Philosophical Magazine*) for lithium fluoride with the specific heat formula $C_v = aT^3+bT^5+cT^7$ (solid line) derived from the results of Clusius and Eichenauer (1956).

known with the same certainty as equation (4). In this paper we shall make the usual assumption of a linear electronic contribution to be added to the lattice specific heat, as predicted by simple theory:

$$C_v = \gamma T+aT^3+bT^5+cT^7+\ldots . \tag{7}$$

As we shall see, the presence of the term γT introduces quite enough uncertainty into the analysis without considering further refinements; but it should be borne in mind that for some solids this assumption may not be justified.

Experimental results on non-insulators are usually analyzed by plotting C_v/T versus T^2 and seeking to draw a straight line through the points in the lowest temperature region. The intercept on the axis at $T^2 = 0$ then gives γ, and the slope of the line gives a and hence Θ_0. This should be reliable if the experiments extend comfortably below $\Theta_D/100$, but otherwise there is the possibility that the true graph versus T^2 of

$$C_v/T = \gamma+aT^2+bT^4+cT^6+\ldots \tag{8}$$

will curve appreciably in the region where the straight line is drawn. Just as such curvature can affect estimates of a and b for an insulator, so here it may affect estimates of γ and a.

There is the occasional instance where the lattice specific heat of a metal $(C_v-\gamma T)$ has been fitted to the form aT^3+bT^5; for example, Dolecek (1955) has done this for specific heat results for lead. Even here, however, care must be taken to avoid a "pseudo" aT^3+bT^5 region; thus Dolecek's line extends up to $\Theta_D/25$ and must therefore for the present be regarded with some suspicion.

(*i*) *White Tin*

Corak and Satterthwaite (1956) have published primary data for the specific heat of white tin in both the normal and superconducting states. Assuming the T^3 law they have fitted the results for the normal state in the range $T < 2.5°$ K. to

$$C_v = 1.75\times10^{-3}T+1943(T/195)^3 \text{ j./mole deg.}; \tag{9}$$

however, there is a small but significant discontinuity in curvature in their plot at 2.5° K. This can be seen more clearly in Fig. 6, which is a plot of $(C_v-\gamma T)/T^3$ versus T^2 with $\gamma = 1.75\times10^{-3}$ j./mole deg.^{2}; here the solid line

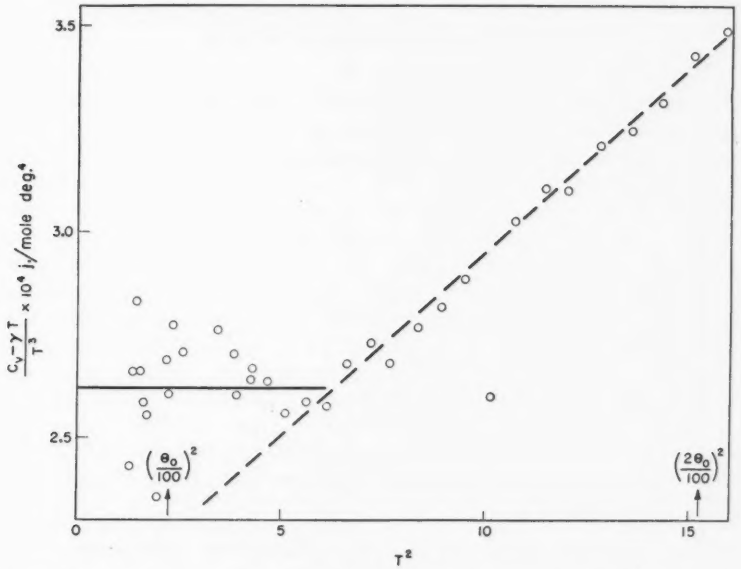

FIG. 6. A graph of $(C_v-\gamma T)/T^3$ versus T^2 for normal white tin—data of Corak and Satterthwaite (1956) with γ taken as 1.75×10^{-3} j./mole deg.^{2}

represents equation (9). It is evident that the results for $T > 2.5°$ K. show an approximate T^5 dependence starting only just above $\Theta_D/100$. It seems likely that this is due mainly to the true bT^5 term, which would then be expected to continue down to $T = 0°$ K. This in turn suggests that the lattice specific heat is being overestimated for $T < 2.5°$ K., and hence that the value of γ chosen is too low. Increasing γ removes the abrupt change in the slope at 2.5° K. and increases the curvature of the graph at low temperatures. Because of uncertainties in the temperature scale at the lowest temperatures it is not possible to fix γ and Θ_0 precisely, but the values $\gamma \sim 1.9\times10^{-3}$ j./mole deg.^{2} and $\Theta_0 \sim 205°$ K. would seem to be fair estimates. This revision makes little difference to Corak and Satterthwaite's subsequent analysis of the properties of the superconducting state.

(*ii*) *Tungsten*

The specific heat of tungsten has been measured in the temperature range 4° to 15° K. by Waite *et al.* (1956). The authors have fitted the results to $1.11\times10^{-3}T+3.60\times10^{-5}T^3$ j./mole deg. over the entire range, which corresponds to a strict T^3 region extending up to $\Theta_D/27$; but they point out that the values between 5° and 8° K. are systematically low by as much as 3%. At the same time it would appear that the results are systematically high just above 8° K. While these deviations may be due to errors in the temperature scale, as the authors suggest, there is the possibility that they are evidence of contributions of terms in T^5 and T^7 to the lattice specific heat. A curve drawn to follow the results closely below 8° K. leads to $\gamma = 1.20\times10^{-3}$ j./mole deg.^{2} and $a = 2.9\times10^{-5}$ j./mole deg.^{4}

(*iii*) *The Noble Metals*

Results of Corak *et al.* (1955) on copper, silver, and gold in the region $T < 4°$ K. suggest that the T^5 term is very small for these metals (4° K. corresponds to $\Theta_0/86$ for copper and to $\Theta_0/41$ for gold). Systematic deviations of the results from linear graphs of C_v/T versus T^2 were observed, but later these were attributed to errors in the temperature scale; certainly terms in T^5 and T^7 cannot account for the deviations, since they occur at the same temperatures for metals of different Θ_0. Kok and Keesom (1936) have measured the specific heat of copper up to 20° K., but unfortunately their experimental error is too great for reliable estimates to be made of the coefficients b and c; even their value of Θ_0, 335° K., seems uncertain. With this value of Θ_0 a graph of $(C_v-aT^3)/T$ versus T^2 indicates a small negative value for b; on the other hand b would not be negative if Θ_0 were taken as 345° K., as found for very pure copper in the more recent experiments (Corak *et al.* 1955; Rayne 1956; Rayne and Kemp 1956). There is, however, some evidence (Rayne 1956) that Θ_0 (and perhaps b also) may not have the same value in specimens of different impurity content.

(*iv*) *Crystals of Diamond Structure*

The published results for the elements of the diamond structure (diamond, silicon, germanium, and gray tin) indicate that the ratios of the coefficients a, b, and c may differ markedly from those for the structures we have considered so far (DeSorbo 1953: diamond; Hill and Parkinson 1952: germanium and gray tin; Keesom and Pearlman 1953*a*: germanium; Pearlman and Keesom 1952: silicon; Webb and Wilks 1955: gray tin). In fact, for germanium, silicon, and tin it appears that there is an abrupt fall-off in Θ_D at temperatures of the order of $\Theta_D/50$. The results for diamond are more anomalous, and it may be that lattices of this structure will provide an interesting subject for both theoretical and experimental work. Unfortunately, primary data have been published only for diamond.

4. SUMMARY

1. Analyses of theoretical models and of experimental results for a number of crystals suggest that in general a strict T^3 dependence of the specific heat

is not to be expected in temperature ranges usually covered in experiments.

2. Specific heat results for insulators at low temperatures can be interpreted most reliably from plots of C_v/T^3 versus T^2.

3. Appreciable deviation from the asymptotic form aT^3+bT^5 of the low temperature expansion for the specific heat will usually occur beyond $T = \Theta_D/50$.

4. Straight line graphs of C_v/T versus T^2 for metals should be viewed with caution, especially if the temperature region covered is small. The graphs should normally be curves because of the contributions of terms in T^5 and T^7 to the lattice specific heat.

APPENDIX

The Diatomic Linear Chain

Following the notation of Blackman (1935*a*) we consider alternate masses M and m; the potential energy between nearest neighbors is $\frac{1}{2}\alpha\delta u^2$, where δu is the difference between the displacements of the atoms from their equilibrium positions. The limiting values of Θ_D at high and low temperatures are then given by

$$\frac{k\Theta_\infty}{h} = \frac{1}{2\pi}\sqrt{\frac{3\alpha(M+m)}{Mm}}, \qquad \frac{k\Theta_0}{h} = \sqrt{\frac{\alpha}{2(M+m)}}. \tag{10}$$

The variation of Θ_D with temperature can be expressed in terms of the parameter $\eta = (M-m)/(M+m)$. At low temperatures we have an expansion in powers of T^2:

$$\Theta_D = \Theta_0[1-\alpha_2(\pi^2T/\Theta_0)^2-\alpha_4(\pi^2T/\Theta_0)^4-\alpha_6(\pi^2T/\Theta_0)^6-\ldots], \tag{11}$$

where

$$\begin{aligned} \alpha_2 &= 0.1+0.3\eta^2, \\ \alpha_4 &= 0.0436+0.8329\eta^2-0.1739\eta^4, \\ \alpha_6 &= 0.0528+3.5608\eta^2-0.4034\eta^4+0.1681\eta^6. \end{aligned} \tag{12}$$

At high temperatures we have an expansion in powers of T^{-2}:

$$\Theta_D = \Theta_\infty\left[1-\beta_2\left(\frac{\Theta_\infty}{T}\right)^2-\beta_4\left(\frac{\Theta_\infty}{T}\right)^4-\ldots\right], \tag{13}$$

where

$$\begin{aligned} \beta_2 &= 10^{-3}(4.17\eta^2-2.50), \\ \beta_4 &= 10^{-6}(2.17\eta^4+82.05\eta^2+0.38). \end{aligned} \tag{14}$$

REFERENCES

BARRON, T. H. K. 1955. Thesis, Oxford University.
BARRON, T. H. K., BERG, W. T., and MORRISON, J. A. 1957. To be published.
BARRON, T. H. K. and DOMB, C. 1955. Proc. Roy. Soc. A, **227**, 447.
BERG, W. T. and MORRISON, J. A. 1957. Proc. Roy. Soc. A (In press).
BHATIA, A. B. and HORTON, G. K. 1955. Phys. Rev. **98**, 1715.
BLACKMAN, M. 1935*a*. Proc. Roy. Soc. A, **148**, 365.
——— 1935*b*. Proc. Roy. Soc. A, **149**, 117.
——— 1937. Proc. Cambridge Phil. Soc. **33**, 94.
——— 1941. Repts. Progr. in Phys. **8**, 11.
——— 1956. Handbuch der Physik, **7**, Pt. 1, 325.

BRISCOE, C. V. and SQUIRE, C. F. 1957. Bull. Am. Phys. Soc. (Ser. II), **2**, 18.
CLUSIUS, K. and EICHENAUER, W. 1956. Z. Naturforsch. **11a**, 715.
CORAK,, W. S., GARFUNKEL, M. P., SATTERTHWAITE, C. B., and WEXLER, A. 1955. Phys. Rev. **98**, 1699.
CORAK, W. S. and SATTERTHWAITE, C. B. 1956. Phys. Rev. **102**, 662.
DESORBO, W. 1953. J. Chem. Phys. **21**, 876.
DOLECEK, R. L. 1955. Conférence de Physique des Basses Temperatures (Annexe 1955–3, Suppl. Bull. Inst. Int. du Froid), p. 300, Paris.
HILL, R. W. and PARKINSON, D. H. 1952. Phil. Mag. (Ser. 7), **43**, 309.
HORTON, G. K. and SCHIFF, H. 1956. Phys. Rev. **104**, 32.
KEESOM, P. H. and PEARLMAN, N. 1953*a*. Phys. Rev. **91**, 1347.
——— 1953*b*. Phys. Rev. **91**, 1354.
KOK, J. A. and KEESOM, W. H. 1936. Physica, **3**, 1035.
DE LAUNAY, J. 1956. J. Chem. Phys. **24**, 1071.
LEIGHTON, R. B. 1948. Revs. Mod. Phys. **20**, 165.
MARTIN, D. L. 1955. Phil. Mag. (Ser. 7), **46**, 751.
PEARLMAN, N. and KEESOM, P. H. 1952. Phys. Rev. **88**, 398.
RAYNE, J. A. 1956. Australian J. Phys. **9**, 189.
RAYNE, J. A. and KEMP, W. R. G. 1956. Australian J. Phys. **9**, 569.
SALTER, L. 1956. Thesis, Oxford University.
WAITE, T. R., CRAIG, R. S., and WALLACE, W. E. 1956. Phys. Rev. **104**, 1240.
WEBB, F. J. and WILKS, J. 1955. Proc. Roy. Soc. A, **230**, 549.

ON THE STRESSES IN TWISTED COMPOSITE SPHERES AND SPHEROIDS[1]

SISIR CHANDRA DAS[2]

ABSTRACT

Stresses have been calculated in the cases of concentric composite elastic spheres and spheroids when they are twisted by couples. The results have been obtained in closed forms.

NOMENCLATURE

u_r, u_θ, u_ϕ = components of displacement in spherical co-ordinates.
u_ξ, u_η, u_ϕ = components of displacement in spheroidal co-ordinates.
ξ, η, ϕ = spheroidal co-ordinates.
r, θ, ϕ = spherical polar co-ordinates.
c = distance of center of spheroid from either focus of generating ellipse.
μ_1 = rigidity of outer material.
μ_2 = rigidity of inner material.
Δ = cubical dilatation.
$\tilde{\omega}_r$, $\tilde{\omega}_\theta$, $\tilde{\omega}_\phi$ = components of rotation in spherical polar co-ordinates.
$\tilde{\omega}_\xi$, $\tilde{\omega}_\eta$, $\tilde{\omega}_\phi$ = components of rotation in spheroidal co-ordinates.
σ_r, σ_θ, σ_ϕ = normal components of stress parallel to directions of r, θ, ϕ.
σ_ξ, σ_η, σ_ϕ = normal components of stress parallel to directions of ξ, η, ϕ.
$\tau_{r\theta}$, $\tau_{r\phi}$, $\tau_{\theta\phi}$ = shear-stress components in spherical co-ordinates.
$\tau_{\xi\eta}$, $\tau_{\xi\phi}$, $\tau_{\eta\phi}$ = shear-stress components in spheroidal co-ordinates.
$1/h_1, 1/h_2, 1/h_3$ = stretch ratios.
A_n, B_n, . . . = constants.

INTRODUCTION

In an earlier paper (Das 1954) the author discussed the case of a small spherical or spheroidal inclusion on the axis of a circular cylinder in torsion. Here similar mathematics has been used to obtain the solutions in the cases of composite spheres and spheroids twisted by couples. The cases of composite materials in cylindrical bars (Das 1955) and truncated cones (Das 1957) due to frictional forces on the curved surfaces have been recently discussed by the author. In this connection it may be mentioned that the torsion problem for composite bars has been dealt with by Muskhelishvili (1953) and also by Payne (1949) and Das (1954).

SPHERES

We take the center of the spheres as the origin, and as the axis of the couple, the axis of z, and use spherical polar co-ordinates. The outer surface

[1]Manuscript received February 21, 1957.
Published by permission of the Deputy Minister, Department of Mines and Technical Surveys, Ottawa. Contributions from the Dominion Observatory, Ottawa, Vol. 3, No. 11.
[2]On study leave of absence from the Department of Mathematics, Chandernagore College, Chandernagore, West Bengal, India.

of the sphere is denoted by $r = a$ and the surface of separation of the two materials by $r = b$.

Assuming $u_r = u_\theta = 0$ and $u_\phi = \omega$, independent of ϕ, we have (Das 1954)

$$(1)\qquad \begin{cases} \Delta = 0, \\ 2\tilde{\omega}_r = \dfrac{1}{r \sin\theta}\dfrac{\partial}{\partial\theta}(\omega \sin\theta), \\ 2\tilde{\omega}_\theta = -\dfrac{1}{r}\dfrac{\partial}{\partial r}(r\omega), \\ 2\tilde{\omega}_\phi = 0. \end{cases}$$

The stress components that do not vanish are given by

$$(2)\qquad \begin{aligned} \tau_{r\phi} &= \mu\left[\frac{\partial\omega}{\partial r} - \frac{\omega}{r}\right], \\ \tau_{\theta\phi} &= \frac{\mu}{r}\left[\frac{\partial\omega}{\partial\theta} - \omega\cot\theta\right]. \end{aligned}$$

Two of the equations of equilibrium (Love 1944) are identically satisfied and the third takes the form

$$(3)\qquad r^2\frac{\partial^2\omega}{\partial r^2} + 2r\frac{\partial\omega}{\partial r} + \frac{\partial}{\partial\theta}\left(\frac{\partial\omega}{\partial\theta} + \omega\cot\theta\right) = 0.$$

The general solution of this equation can be taken as

$$(4)\qquad \omega = \sum\left(A_n r^n + \frac{B_n}{r^{n+1}}\right)\frac{d}{d\theta}[P_n(\cos\theta)],$$

where A_n and B_n are constants and P_n denotes Legendre's function of the first kind and of degree n.

If the tractions on the hemisphere $z > 0$ are statically equivalent to a couple of moment $\frac{1}{2}\pi a^3 S$, a being the radius of the sphere, and if for $z < 0$ the tractions are statically equivalent to an equal couple about the same axis but in the opposite sense, then the boundary conditions may be taken as

$$(5)\qquad \begin{cases} (\tau_{r\phi})_1 = S\sin\theta\cos\theta & \text{at } r = a, \\ (\tau_{r\phi})_1 = (\tau_{r\phi})_2 & \text{at } r = b, \\ \omega_1 = \omega_2 & \text{at } r = b, \end{cases}$$

where the suffixes 1 and 2 denote stresses and displacements for the outer material and the inner material respectively.

For a solution suitable for our problem we take

$$(6)\qquad \begin{aligned} \omega_1 &= \left(A_2 r^2 + \frac{B_2}{r^3}\right)\frac{d}{d\theta}[P_2(\cos\theta)], \\ \omega_2 &= A_2' r^2 \frac{d}{d\theta}[P_2(\cos\theta)]. \end{aligned}$$

The boundary conditions (5) will be satisfied if

$$(7)\qquad \begin{cases} A_2 = \dfrac{Sa^4(\mu_2+4\mu_1)}{3\mu_1[4(\mu_1-\mu_2)b^5-(\mu_2+4\mu_1)a^5]}, \\ B_2 = \dfrac{S\,a^4b^5(\mu_1-\mu_2)}{3\mu_1[4(\mu_1-\mu_2)b^5-(\mu_2+4\mu_1)a^5]}, \\ A_2' = \dfrac{5Sa^4}{3[4(\mu_1-\mu_2)b^5-(\mu_2+4\mu_1)a^5]}, \end{cases}$$

where μ_1 and μ_2 are the rigidities for the outer and inner spheres respectively.

The stresses on the surface of separation are calculated to be

$$(8)\qquad \begin{aligned} (\tau_{r\phi})_{r=b} &= -\frac{5Sa^4b\mu_2\cos\theta\sin\theta}{[4(\mu_1-\mu_2)b^5-(\mu_2+4\mu_1)a^5]}, \\ (\tau_{\theta\phi})_{r=b} &= -\frac{5Sa^4b\mu_1\sin^2\theta}{[4(\mu_1-\mu_2)b^5-(\mu_2+4\mu_1)a^5]}. \end{aligned}$$

PROLATE SPHEROID

Here we take the center of the spheroid as origin and using the transformation

$$(9)\qquad \begin{cases} x = c\sinh\xi\sin\eta\cos\phi, \\ y = c\sinh\xi\sin\eta\sin\phi, \\ z = c\cosh\xi\cos\eta, \end{cases}$$

we find that ξ = constant gives confocal prolate spheroids which can be written as

$$(10)\qquad \frac{z^2}{c^2\cosh^2\xi}+\frac{x^2+y^2}{c^2\sinh^2\xi}=1.$$

The outer surface is denoted by $\xi=\alpha$, while the surface of separation of the two materials is taken as $\xi=\beta$.

Taking the displacement components $u_\xi = u_\eta = 0$ and $u_\phi = \omega$, independent of ϕ, i.e., a function of ξ and η only, we have

$$(11)\qquad \begin{cases} \Delta = 0, \\ 2\tilde{\omega}_\xi = h_2h_3\dfrac{\partial}{\partial\eta}\left(\dfrac{\omega}{h_3}\right), \\ 2\tilde{\omega}_\eta = -h_3h_1\dfrac{\partial}{\partial\xi}\left(\dfrac{\omega}{h_3}\right), \\ 2\tilde{\omega}_\phi = 0, \end{cases}$$

where

$$(12)\qquad \begin{aligned} \frac{1}{h_1^2} &= \frac{1}{h_2^2} = c^2(\cosh^2\xi-\cos^2\eta), \\ \frac{1}{h_3^2} &= c^2\sinh^2\xi\sin^2\eta. \end{aligned}$$

The equations of equilibrium that do not vanish identically can be written as

$$(13)\qquad \frac{\partial}{\partial\xi}\left(\frac{\partial\omega}{\partial\xi}+\omega\coth\xi\right)+\frac{\partial}{\partial\eta}\left(\frac{\partial\omega}{\partial\eta}+\omega\cot\eta\right)=0,$$

the solution of which can be taken as

$$\omega = \left[A\frac{d}{d\xi}\{P_2(\cosh\xi)\} + B\frac{d}{d\xi}\{Q_2(\cosh\xi)\}\right]\frac{d}{d\eta}\{P_2(\cos\eta)\}, \tag{14}$$

where P_2 and Q_2 are the Legendre functions of the second degree and of the first and second kind respectively.

The stresses that do not vanish are given by

$$\begin{aligned}\tau_{\xi\phi} = \frac{\mu}{c(\cosh^2\xi-\cos^2\eta)^{\frac{1}{2}}}\Bigg\{&A_2\left[\frac{d^2[P_2(\cosh\xi)]}{d\xi^2} - \coth\xi\,\frac{d[P_2(\cosh\xi)]}{d\xi}\right]\\ &+ B_2\left[\frac{d^2[Q_2(\cosh\xi)]}{d\xi^2} - \coth\xi\,\frac{d[Q_2(\cosh\xi)]}{d\xi}\right]\Bigg\}\frac{d}{d\eta}[P_2(\cos\eta)],\\ \tau_{\eta\phi} = \frac{3\mu\sin^2\eta}{c(\cosh^2\xi-\cos^2\eta)^{\frac{1}{2}}}&\left[A_2\frac{d[P_2(\cosh\xi)]}{d\xi} + B_2\frac{d[Q_2(\cosh\xi)]}{d\xi}\right].\end{aligned} \tag{15}$$

When the tractions on the half of the spheroid for which $0 < \eta < \frac{1}{2}\pi$ are statically equivalent to a couple of moment $\frac{1}{2}\pi c^3\sinh^2\alpha.S$ and the tractions on the other half (for $\frac{1}{2}\pi < \eta < \pi$) are statically equivalent to an equal and opposite couple about the same axis, we can take as boundary condition

$$\tau_{\xi\phi} = -\frac{S\sin\eta\cos\eta}{(\cosh^2\alpha-\cos^2\eta)^{\frac{1}{2}}} \text{ at } \xi = \alpha. \tag{16}$$

The other boundary conditions are obtained from the continuity of the stresses and the displacement at the surface of separation, which can be written as

$$\begin{aligned}(\tau_{\xi\phi})_1 &= (\tau_{\xi\phi})_2,\\ \omega_1 &= \omega_2, \qquad \text{at } \xi = \beta,\end{aligned} \tag{17}$$

where suffixes 1 and 2 denote the stresses and displacements for the outer material and the inner material respectively.

As a solution suitable for the problem we take

$$\begin{aligned}\omega_1 &= \left[A_1\frac{d}{d\xi}\{P_2(\cosh\xi)\}\right]\frac{d}{d\eta}\{P_2(\cos\eta)\},\\ \omega_2 &= \left[A_2\frac{d}{d\xi}\{P_2(\cosh\xi)\} + B_2\frac{d}{d\xi}\{Q_2(\cosh\xi)\}\right]\frac{d}{d\eta}\{P_2(\cos\eta)\}.\end{aligned} \tag{18}$$

The conditions (16) and (17) will be satisfied if

$$\left\{\begin{aligned}A_1 &= \frac{cS}{9}\frac{(G+H)}{[(\mu_1-\mu_2)F+\sinh^2\alpha(\mu_1G+\mu_2H)]},\\ A_2 &= \frac{cS}{9\mu_1}\frac{(\mu_1G+\mu_2H)}{[(\mu_1-\mu_2)F+\sinh^2\alpha(\mu_1G+\mu_2H)]},\\ B_2 &= \frac{cS}{3\mu_1}\frac{(\mu_1-\mu_2)\cosh^2\beta\sinh^2\beta}{[(\mu_1-\mu_2)F+\sinh^2\alpha(\mu_1G+\mu_2H)]},\end{aligned}\right. \tag{19}$$

where

$$(20)\qquad \begin{cases} F = \sinh^2\beta\cosh^2\beta\left[6Q_2(\cosh\alpha)-2\dfrac{d^2}{d\alpha^2}\{Q_2(\cosh\alpha)\}\right], \\ G = \cosh^2\beta\left[6Q_2(\cosh\beta)-2\dfrac{d^2}{d\beta^2}\{Q_2(\cosh\beta)\}\right], \\ H = \sinh^2\beta\left[6Q_2(\cosh\beta)-\dfrac{d^2}{d\beta^2}\{Q_2(\cosh\beta)\}\right], \end{cases}$$

μ_1 and μ_2 being the rigidities of the outer and the inner material respectively.

The stresses on the surface of separation are as follows:

$$(21)\qquad \begin{aligned} \tau_{\xi\phi} &= -\frac{\mu_1\mu_2 S\sinh^2\beta(G+H)\sin\eta\cos\eta}{(\cosh^2\beta-\cos^2\eta)^{\frac{1}{2}}[(\mu_1-\mu_2)F+\sinh^2\alpha(\mu_1 G+\mu_2 H)]}, \\ \tau_{\eta\phi} &= \frac{\mu_1 S\sinh\beta\cosh\beta(G+H)\sin^2\eta}{(\cosh^2\beta-\cos^2\eta)^{\frac{1}{2}}[(\mu_1-\mu_2)F+\sinh^2\alpha(\mu_1 G+\mu_2 H)]}. \end{aligned}$$

OBLATE SPHEROID

Using the transformation

$$(22)\qquad \begin{cases} x = c\sinh\xi\sin\eta\cos\phi, \\ y = c\sinh\xi\sin\eta\sin\phi, \\ z = c\cosh\xi\cos\eta, \end{cases}$$

we get for different values of ξ confocal oblate spheroids given by

$$(23)\qquad \frac{x^2+y^2}{c^2\cosh^2\xi}+\frac{z^2}{c^2\sinh^2\xi}=1.$$

Taking $\mu_\xi = \mu_\eta = 0$ and the azimuthal component ω independent of ϕ we get the only equation of equilibrium that does not identically vanish in the form

$$(24)\qquad \frac{\partial}{\partial\xi}\left[\frac{\partial\omega}{\partial\xi}+\omega\tanh\xi\right]+\frac{\partial}{\partial\eta}\left[\frac{\partial\omega}{\partial\eta}+\omega\cot\eta\right]=0.$$

As solution to it we can write

$$(25a)\qquad \omega_1 = \left[A_1'\frac{d}{d\xi}\{P_2(i\sinh\xi)\}\right]\frac{d}{d\eta}\{P_2(\cos\eta)\}$$

for the inner material and

$$(25b)\quad \omega_2 = \left[A_2'\frac{d}{d\xi}\{P_2(i\sinh\xi)\}+B_2'\frac{d}{d\xi}\{Q_2(i\sinh\xi)\}\right]\frac{d}{d\eta}\{P_2(\cos\eta)\}$$

for the outer ($i=\sqrt{-1}$).

When the tractions on the half of the spheroid for which $0<\eta<\frac{1}{2}\pi$ are statically equivalent to a couple of moment $\frac{1}{2}\pi c^3\cosh^2\alpha.S$ and the tractions on the other half produce an equal and opposite couple about the same axis, we get

$$(26)\qquad (\tau_{\xi\phi})_1 = -S\frac{\sin\eta\cos\eta}{(\cosh^2\alpha-\sin^2\eta)}\quad \text{at } \xi=\alpha,$$

while the other boundary conditions are as in the previous cases, i.e. at $\xi=\beta$

$$(\tau_{\xi\phi})_1 = (\tau_{\xi\phi})_2, \tag{27}$$

$$\omega_1 = \omega_2.$$

These conditions, (26) and (27), are satisfied if

$$\left\{\begin{aligned} A_1' &= \frac{cS}{9}\frac{(G'+H')}{[(\mu_1-\mu_2)F'+\cosh^2\alpha(\mu_1G'+\mu_2H')]}, \\ A_2' &= \frac{cS}{9\mu_1}\frac{(\mu_1G'+\mu_2H')}{[(\mu_1-\mu_2)F'+\cosh^2\alpha(\mu_1G'+\mu_2H')]}, \\ B_2' &= -\frac{cS}{3\mu_1}\frac{(\mu_1-\mu_2)\cosh^2\beta\sinh^2\beta}{[(\mu_1-\mu_2)F'+\cosh^2\alpha(\mu_1G'-\mu_2H')]}, \end{aligned}\right. \tag{28}$$

where

$$\left\{\begin{aligned} F' &= \sinh^2\beta\cosh^2\beta\left[6Q_2(i\sinh\alpha)-2\frac{d^2}{d\alpha^2}\{Q_2(i\sinh\alpha)\}\right], \\ G' &= \sinh^2\beta\left[6Q_2(i\sinh\beta)-2\frac{d^2}{d\beta^2}\{Q_2(i\sinh\beta)\}\right], \\ H' &= \cosh^2\beta\left[6Q_2(i\sinh\beta)-\frac{d^2}{d\beta^2}\{Q_2(i\sinh\beta)\}\right], \end{aligned}\right. \tag{29}$$

μ_1 and μ_2 being the rigidities of the outer and inner material respectively.

The stresses in this case at the surface of separation, i.e. at $\xi = \beta$, are given by

$$\begin{aligned} \tau_{\xi\phi} &= -\frac{\mu_1\mu_2 S\cosh^2\beta(G'+H')\sin\eta\cos\eta}{(\cosh^2\beta-\cos^2\eta)^{\frac{1}{2}}[(\mu_1-\mu_2)F'+\cosh^2\alpha(\mu_1G'+\mu_2H')]}, \\ \tau_{\eta\phi} &= \frac{\mu_1 S\sinh\beta\cosh\beta(G'+H')\sin^2\eta}{(\cosh^2\beta-\cos^2\eta)^{\frac{1}{2}}[(\mu_1-\mu_2)F'+\cosh^2\alpha(\mu_1G'+\mu_2H')]}. \end{aligned} \tag{30}$$

DISCUSSION

The stresses in the cases of thick spherical shells and spheroidal shells with confocal surfaces can be easily deduced by putting $\mu_2 = 0$ in the expressions for stresses. Thus we have in the case of a spherical shell

$$\begin{aligned} (\tau_{r\phi})_{r=b} &= 0, \\ (\tau_{\theta\phi})_{r=b} &= \frac{5}{4}\frac{Sa^4b\sin^2\theta}{b^5-a^5}. \end{aligned} \tag{31}$$

In the case of a prolate spheroidal shell

$$\begin{aligned} (\tau_{\xi\phi})_{\xi=\beta} &= 0, \\ (\tau_{\eta\phi})_{\xi=\beta} &= \frac{S\cdot\sinh\beta\cosh\beta(G+H)\sin^2\eta}{(\cosh^2\beta-\cos^2\eta)^{\frac{1}{2}}[F+G\cosh^2\alpha]}, \end{aligned} \tag{32}$$

and in the case of an oblate spheroidal shell

$$\begin{aligned} (\tau_{\xi\phi})_{\xi=\beta} &= 0, \\ (\tau_{\eta\phi})_{\xi=\beta} &= \frac{S\cdot\sinh\beta\cosh\beta(G'+H')\sin^2\eta}{(\cosh^2\beta-\cos^2\eta)^{\frac{1}{2}}[F'+G'\cosh^2\alpha]}. \end{aligned} \tag{33}$$

When the inner material is perfectly rigid we have $\mu_2 \to \infty$, and in that case for the spherical shell we have

$$(\tau_{r\phi})_{r=b} = \frac{5}{4} S \frac{a^4 b \sin\theta \cos\theta}{(a^5+b^5)}, \qquad (\tau_{\theta\phi})_{r=b} = 0. \tag{34}$$

In the similar case for a prolate spheroidal shell we have

$$(\tau_{\xi\phi})_{\xi=\beta} = \frac{\mu_1 S \sinh^2\beta(G+H)\sin\eta\cos\eta}{(\cosh^2\beta-\cos^2\eta)^{\frac{1}{2}}[F-H\sinh^2\alpha]}, \qquad (\tau_{\eta\phi})_{\xi=\beta} = 0, \tag{35}$$

whereas in the case of an oblate spheroidal shell we get

$$(\tau_{\xi\phi})_{\xi=\beta} = \frac{\mu_1 S\cdot\cosh^2\beta(G'+H')\sin\eta\cos\eta}{(\cosh^2\beta-\cos^2\eta)^{\frac{1}{2}}[F'-H'\cos^2\alpha]}, \qquad (\tau_{\eta\phi})_{\xi=\beta} = 0. \tag{36}$$

ACKNOWLEDGMENTS

The author offers his sincere thanks to Dr. B. Sen for his kind help in the preparation of this paper. The author is also indebted to the National Research Council of Canada for the award of a Postdoctorate Fellowship and wishes to thank Dr. J. H. Hodgson, Head, Seismology Division of the Dominion Observatory at Ottawa, for his interest and encouragement.

REFERENCES

DAS, S. C. 1954. J. Appl. Mechanics, **21**, No. 1.
——— 1955. Proc. 1st Congr. Theoret. and Appl. Mechanics, India.
——— 1956. Silver Jubilee Commemoration Volume of Chandernagore College, Chandernagore, India (In press).
——— 1957. Indian J. Theoret. Phys. (In press).
LOVE, A. E. H. 1944. A treatise on mathematical theory of elasticity (Dover Publications, New York, N.Y.).
MUSKHELISHVILI, N. I. 1953. Some basic problems of the mathematical theory of elasticity, English Translation by J. R. M. Radok (P. Noordhoff Ltd., Groningen, Holland), p. 605.
PAYNE, L. E. 1949. Iowa State College J. Sci. **23**, 381.

NOTES

AN ATTEMPT TO DETECT INFRARED ABSORPTION IN LIQUID HELIUM

D. C. Baird, M. H. Edwards, and G. Fleming

The infrared absorption in liquid helium has been investigated at wavelengths from 1 to 4 μ using a Beckman IR-2 Infrared Spectrophotometer and a metal cryostat designed for other optical experiments on liquid helium (Edwards 1956). To our knowledge no such measurements have been made previously, either above or below the λ-point (2.1735° K.).

The sample space of the IR-2 was lengthened by moving the light source unit back about 15 inches from the monochromator and energy receiver unit so that the cryostat, containing the optical cell, could be placed between these two units. The sodium chloride end windows of the two units were protected by thin glass covers. The beam also passed through the outer windows of the cryostat, consisting of about 2 mm. of glass, and through two 5 mm. thick fused silica windows at the ends of the helium cell. The over-all reduction in intensity after these modifications was a factor of about 4 over most of the wavelength range. The 9.58 cm. long copper cell with fused silica end windows was surrounded by a liquid helium bath whose temperature was controlled by a manostat and measured by reading the vapor pressure (Clement *et al.* 1955) above the bath. The cell could be filled separately by condensation of pure helium gas, purified by passing through a liquid-air-cooled charcoal trap.

The experimental procedure involved a series of four consecutive runs at liquid helium temperatures. After the helium bath was filled with liquid helium, the absorbances at some 80 wavelengths from 1.0 to 4.0 μ were read for each of the following conditions:

1. Cell evacuated, bath temperature about 3° K.
2. Cell filled with liquid helium at 60 p.s.i.g., at 2.068° K.
3. Cell filled with liquid helium at 60 p.s.i.g., at 4.216° K.
4. Cell evacuated, bath temperature at 4.216° K.

The effective band width ranged from about 0.015 μ or 160 cm^{-1} at 1 μ to 0.2 μ or 130 cm^{-1} at 4 μ.

During the 3 hours of this experiment the gain of the amplifier altered slightly, so that run 4 gave absorbances about 0.015 higher than run 1. After this drift is taken into account no absorption of infrared radiation by liquid helium from 1.0 to 4.0 μ is apparent either above or below the λ-point. (We can say nothing about the region from 2.65 to 2.85 μ, however, because of the presence of a sharp absorption peak in the fused silica.) We believe we could have detected a change in absorbance of as little as 0.015, corresponding to a decrease in transmittance through our cell of about 3.5%, or a mass

absorption coefficient of 0.024 cm.²/g. at 2.068° K. or 0.026 cm.²/g. at 4.216° K. We conclude, therefore, that if there is any infrared absorption by liquid helium, it must be less than these amounts.

ACKNOWLEDGMENTS

It is a pleasure to acknowledge the support of the Defence Research Board (Grant No. DRB 9510-10). The authors also wish to thank Dr. W. R. Sawyer for making the IR-2 spectrophotometer available to them.

CLEMENT, J. R., LOGAN, J. K., and GAFFNEY, J. 1955. Phys. Rev. **100**, 743 (Note added in proof).
EDWARDS, M. H. 1956. Can. J. Phys. **34**, 898.

RECEIVED MARCH 4, 1957.
ROYAL MILITARY COLLEGE,
KINGSTON, ONTARIO.

SPONTANEOUS MAGNETIZATION IN Mn–Ga–C ALLOYS

H. P. MYERS*

In the ternary alloy systems Mn–Al–C, Mn–Zn–C, Mn–Sn–C, and Mn–In–C there occurs a distinctive face-centered cubic ternary phase. This phase exists over a wide range of composition and shows structural order which for the Al and Zn ternary alloys is complete at the compositions $Mn_{60}Al_{20}C_{20}$ and $Mn_{60}Zn_{20}C_{20}$. The phase has pronounced spontaneous magnetization, which in general may be attributed to ferromagnetism although ferrimagnetic properties are also found in certain Zn alloys (Butters and Myers 1955; Brockhouse and Myers 1957). Recently it has been found that a similar magnetic ternary phase also occurs in the Mn–Ga–C system.

Small melts of Mn–Ga–C alloys were made using induction heating in an argon atmosphere. The melts were annealed to produce homogeneous structures and then investigated using techniques already described (Butters and Myers 1955). The gallium used had purity better than 99.9%, the manganese and graphite being similar to those used in previous work.

Single-phase alloys were found over the range 10–18% Ga;† they were hard and brittle. X-Ray and magnetic data obtained on four alloys lying in the above composition range are given in Table I. The X-ray powder photographs showed the extra diffraction lines typical of the ordered structure found in the alloys $Mn_{60}Zn_{20}C_{20}$ and $Mn_{60}Al_{20}C_{20}$. A pronounced spontaneous magnetization was found in all the alloys studied, the σ–T curves being typical of ferromagnetic substances; the curve for an alloy of composition

*Now with AB Atomenergi, Stockholm, Sweden.

†Compositions are expressed in atomic percentage. Only nominal compositions are given but we believe that the maximum deviation in either Mn or Ga contents would not be greater than ±½%. The carbon content was always held nominally at 20%, and any deviation here would probably be to lower carbon contents but again the deviation should not be greater than ½%.

TABLE I

SOME PROPERTIES OF Mn–Ga–C ALLOYS

Composition	σ_0, ° K.	Curie temp., ° K.	Bohr magneton value	Lattice parameter, Å
$Mn_{62}Ga_{18}C_{20}$	90	390	1.27	3.876
$Mn_{63}Ga_{18}C_{20}$	77.5	534	1.04	3.874
$Mn_{67}Ga_{13}C_{20}$	63	—	0.82	3.879
$Mn_{70}Ga_{10}C_{20}$	51	—	0.62	3.881

$Mn_{62}Ga_{18}C_{20}$ is reproduced in Fig. 1. As the gallium content is reduced the magnetization decreases but the Curie temperature increases. The alloy

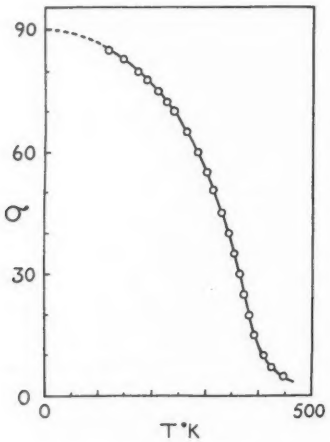

FIG. 1. Variation of saturation magnetization (H = 16,200 oersteds) with temperature for the alloy $Mn_{62}Ga_{18}C_{20}$.

compositions listed in Table I are the nominal values; however, on account of the low melting point and wetting property of gallium, they were easily prepared and we believe the actual alloy compositions were close to the nominal values. Bohr magneton numbers per manganese atom were therefore calculated, and the variation of this quantity with composition is shown in Fig. 2.

The structure and variation of lattice parameter of the Mn–Ga–C ternary phase are very similar to those observed for the Mn–Al–C alloys. In both these ternary phases the lattice parameter varies very little with the relative Mn:Ga or Mn:Al contents; furthermore the actual values of lattice parameter in the two alloy series differ at the most by only 0.005 Å.* Our magnetic apparatus was arranged for low temperature measurements and for this

*The alloy $Mn_{60}Al_{20}C_{20}$ is a possible exception. It appears to have a significantly smaller lattice parameter than Al alloys with greater manganese content; for the latter the lattice parameters are essentially independent of composition.

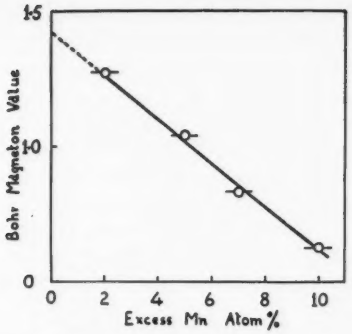

FIG. 2. Variation of Bohr magneton number per manganese atom with composition for Mn–Ga–C alloys.

reason it was not practicable to measure the Curie temperatures of the two alloys with the lower gallium contents; the Curie temperatures which were determined, however, are very close to those of Mn–Al–C alloys of similar composition.

The Bohr magneton values per manganese atom do differ, being 1.26 for $Mn_{60}Al_{20}C_{20}$ and 1.42 for $Mn_{60}Ga_{20}C_{20}$. The latter value is obtained by extrapolation from Fig. 2 since an alloy of the optimum composition for maximum structural order was not stable. We do not consider that the whole of this difference in the magneton values can be attributed to uncertainty in the alloy compositions. Recent measurements on alloys of the form $Mn_{60}Zn_xAl_{20-x}C_{20}$ (Howe and Myers 1957) show that the magnetization of these alloys is not governed by a simple valency mechanism. There is therefore no strong experimental evidence which demands exactly similar manganese moments in the ternary phases with Al and with Ga. The variation of Bohr magneton number with composition can be given a simple representation of the form

$$(60+C)\mu_C = 60\mu_1 + C\mu_2,$$

where μ_C = mean moment per Mn atom in an alloy containing $60+C$ atom per cent manganese;

μ_1 = mean moment per Mn atom in $Mn_{60}Ga_{20}C_{20}$, i.e. of Mn atoms in face center positions; this is assumed independent of composition;

μ_2 = mean moment per Mn atom replacing Ga in the unit cell—i.e. at a cube corner position, including any effect due to the removal of the Ga atom.

The results of Fig. 2 are well represented by the above expression if $\mu_2 = 4\pm 0.3\mu_B$. Similarly the properties of the Zn and Al alloys may be given the same representation if in these cases $\mu_2 = 4.0\pm 0.2\mu_B$ and $4.5\pm 0.5\mu_B$ respectively. The poorer result for the Al alloys results from the limited range of composition for which measurements are available. It is not clear how this representation is to be interpreted. Thus the different magnetic moments found for the manganese atoms in $Mn_{60}Al_{20}C_{20}$, $Mn_{60}Zn_{20}C_{20}$, and $Mn_{60}Ga_{20}C_{20}$ must be

attributed to the atoms Al, Zn, and Ga which distinguish the alloys; on the other hand the replacement of an Al, Zn, or Ga atom by one of manganese appears to give rise to a similar decrease in average magnetic moment in each alloy system.

Unfortunately these ternary phases in the Mn–In–C and Mn–Sn–C systems are stable only in composition ranges widely different from those in which the Zn, Al, and Ga ternary phases occur; the data are therefore not comparable. Even so the Sn and In alloys, although far removed from the optimum composition for complete structural order, nevertheless show such order and the occurrence and persistence of structural order over wide ranges of both composition and temperature has not been satisfactorily explained.

ACKNOWLEDGMENTS

The author wishes to acknowledge the assistance of Mr. R. G. Butters with the experimental work and the financial assistance of the Defence Research Board of Canada (Project No. D 44–95–35–02) and the National Research Council of Canada.

BUTTERS, R. G. and MYERS, H. P. 1955. Phil. Mag. **46**, 132, 895.
BROCKHOUSE, B. N. and MYERS, H. P. 1957. Can. J. Phys. **35**, 313.
HOWE, L. and MYERS, H. P. 1957. Phil. Mag. (To be published).

RECEIVED MARCH 4, 1957.
DEPARTMENT OF MINING AND METALLURGY,
UNIVERSITY OF BRITISH COLUMBIA,
VANCOUVER, B.C.

CANADIAN JOURNAL OF PHYSICS

Notes to Contributors

Manuscripts

(i) **General.** Manuscripts, in English or French, should be typewritten, double spaced, on paper $8\frac{1}{2}\times11$ in. **The original and one copy are to be submitted.** Tables and captions for the figures should be placed at the end of the manuscript. Every sheet of the manuscript should be numbered.

Style, arrangement, spelling, and abbreviations should conform to the usage of this journal. Names of all simple compounds, rather than their formulas, should be used in the text. Greek letters or unusual signs should be written plainly or explained by marginal notes. Superscripts and subscripts must be legible and carefully placed.

Manuscripts and illustrations should be carefully checked before they are submitted. Authors will be charged for unnecessary deviations from the usual format and for changes made in the proof that are considered excessive or unnecessary.

(ii) **Abstract.** An abstract of not more than about 200 words, indicating the scope of the work and the principal findings, is required, except in Notes.

(iii) **References.** References should be listed **alphabetically by authors' names,** unnumbered, and typed after the text. The form of the citations should be that used in current issues of this journal; in references to papers in periodicals, titles should not be given and only initial page numbers are required. The names of periodicals should be abbreviated in the form given in the most recent *List of Periodicals Abstracted by Chemical Abstracts*. All citations should be checked with the original articles and each one referred to in the text by the authors' names and the year.

(iv) **Tables.** Tables should be numbered in roman numerals and each table referred to in the text. Titles should always be given but should be brief; column headings should be brief and descriptive matter in the tables confined to a minimum. Vertical rules should be used only when they are essential. Numerous small tables should be avoided.

Illustrations

(i) **General.** All figures (including each figure of the plates) should be numbered consecutively from 1 up, in arabic numerals, and each figure referred to in the text. The author's name, title of the paper, and figure number should be written in the lower left corner of the sheets on which the illustrations appear. Captions should not be written on the illustrations (see Manuscripts (i)).

(ii) **Line Drawings.** Drawings should be carefully made with India ink on white drawing paper, blue tracing linen, or co-ordinate paper ruled in blue only; any co-ordinate lines that are to appear in the reproduction should be ruled in black ink. Paper ruled in green, yellow, or red should not be used unless it is desired to have all the co-ordinate lines show. All lines should be of sufficient thickness to reproduce well. Decimal points, periods, and stippled dots should be solid black circles large enough to be reduced if necessary. Letters and numerals should be neatly made, preferably with a stencil (**do NOT use typewriting**) and be of such size that the smallest lettering will be not less than 1 mm. high when reproduced in a cut 3 in. wide.

Many drawings are made too large; originals should not be more than 2 or 3 times the size of the desired reproduction. In large drawings or groups of drawings the ratio of height to width should conform to that of a journal page but the height should be adjusted to make allowance for the caption.

The original drawings and one set of clear copies (e.g. small photographs) are to be submitted.

(iii) **Photographs.** Prints should be made on glossy paper, with strong contrasts. They should be trimmed so that essential features only are shown and mounted carefully, with rubber cement, on white cardboard with no space or only a **very** small space (less than 1 mm.) between them. In mounting, full use of the space available should be made (to reduce the number of cuts required) and the ratio of height to width should correspond to that of a journal page ($4\frac{3}{4}\times7\frac{1}{2}$ in.); however, allowance must be made for the captions. Photographs or groups of photographs should not be more than 2 or 3 times the size of the desired reproduction.

Photographs are to be submitted in duplicate; if they are to be reproduced in groups one set should be mounted, the duplicate set unmounted.

Reprints

A total of 50 reprints of each paper, without covers, are supplied free. Additional reprints, with or without covers, may be purchased.

Charges for reprints are based on the number of printed pages, which may be calculated approximately by multiplying by 0.6 the number of manuscript pages (double-spaced typewritten sheets, $8\frac{1}{2}\times11$ in.) and including the space occupied by illustrations. An additional charge is made for illustrations that appear as coated inserts. The cost per page is given on the reprint requisition which accompanies the galley.

Any reprints required in addition to those requested on the author's reprint requisition form must be ordered officially as soon as the paper has been accepted for publication.

Contents

Printed in Canada *by* University of Toronto Press